



A cartography of spatial relationships in a symbolic image database

Nguyen Vu Hoang, Valérie Gouet-Brunet, Marta Rukoz

► To cite this version:

Nguyen Vu Hoang, Valérie Gouet-Brunet, Marta Rukoz. A cartography of spatial relationships in a symbolic image database. 2011. hal-00875555

HAL Id: hal-00875555

<https://hal.science/hal-00875555>

Preprint submitted on 22 Oct 2013

HAL is a multi-disciplinary open access archive for the deposit and dissemination of scientific research documents, whether they are published or not. The documents may come from teaching and research institutions in France or abroad, or from public or private research centers.

L'archive ouverte pluridisciplinaire **HAL**, est destinée au dépôt et à la diffusion de documents scientifiques de niveau recherche, publiés ou non, émanant des établissements d'enseignement et de recherche français ou étrangers, des laboratoires publics ou privés.

CAHIER DU LAMSADE

309

Mai 2011

A cartography of spacial relationships in a symbolic
image database

Nguyen Vu Hoang, Valérie Gouet-Brunet, Marta Rukoz

LAMSADE Research Report n° XXX

A cartography of spatial relationships in a symbolic image database

Nguyen Vu Hoang^{1,2}, Valérie Gouet-Brunet², Marta Rukoz^{1,3}

1 : LAMSADE - Université Paris-Dauphine - Place de Lattre de Tassigny - F75775 Paris Cedex 16

2 : CEDRIC/CNAM - 292, rue Saint-Martin - F75141 Paris Cedex 03

3 : Université Paris Ouest Nanterre La Défense - 200, avenue de la République - F92001 Nanterre Cedex

`nguyenvu.hoang@dauphine.fr`, `valerie.gouet@cnam.fr`, `marta.rukoz@dauphine.fr`

18 avril 2011

Abstract

This work addresses the problem of the representation of spatial relationships between symbolic objects in images. We have studied the distribution of several categories of relationships in LabelMe¹, a public database of images where objects are annotated manually and online by users. Our objective is to build a cartography of the spatial relationships that can be encountered in a representative database of images of heterogeneous content, with the main aim of exploiting it in future applications of Content-Based Image Indexing (CBIR), such as object recognition or retrieval. In this paper, we present the framework of the experiments made and give an overview of the main results obtained, as an introduction to the website ¹ dedicated to this work, whose ambition is to make available all these statistics to the CBIR community.

1 Introduction

We are interested in the representation of spatial relationships between symbolic objects in images. In CBIR, embedding such information into image content description provides a better representation of the content as well as new scenarios of interrogation. Literature on spatial relationships is very rich - several hundreds of papers exist on this topic - and a lot of approaches were proposed (see for example the survey [4]). Most of them describe different aspects of spatial relationships, e.g. directional [7] or topological [3] relationships, and have been evaluated on small synthetic or specific image datasets, e.g. medical or satellite imagery. In this work, we propose to build a cartography of the spatial relationships that can be encountered in a database of images of heterogeneous natural contents, such as audiovisual, web or family visual contents. We have chosen a public annotated database, from the platform LabelMe¹, which is described in section 2. This cartography collects statistical informations on the trends of spatial relationships involving symbolic objects effectively encountered in this database, with

1. LabelMe : <http://labelme.csail.mit.edu>.

the aim of exploiting them in future CBIR applications, for improving tasks such as object recognition or retrieval. Here, we focus on the analysis of unary, binary, and ternary relationships. We present the results of this analysis, which are made available to the CBIR community on our website².

This report is organized as follows : In Section 2, we introduce the LabelMe image database used in our work and objects categories extracted from it. Section 3, 4, and 5 are respectively dedicated to the statistical studies on unary, binary and ternary relationship. Finally, a conclusion of this work to finish the report is presented in Section 6.

2 Annotated image database

2.1 Studied database

LabelMe [12] is a platform containing image databases and an online annotation tool that allows users to indicate freely, by constructing a polygon and a label, the many objects depicted in a image as they wish. Thus, each object, called entity in this work, is presented by a polygon and a label. In our work, each label is considered as the name of an entity category, so all entities possessing the same label belong to a same category. We used one of the test databases of this platform which contains 1133 annotated images in daily contexts (see examples in Fig.1 and Fig.2). The content of these images is very heterogeneous, it contains many categories and many images, and it is not specific to a particular domain. Therefore, studying this database can provide a general view about categories and their relationships, and the results should not be influenced noticeably by changing the database.

In order to guarantee the quality of the database we verified carefully each annotated image for consistency :

- Firstly, we manually consolidated synonymous labels by correcting orthographic mistakes and merging labels having the same meaning.
- Secondly, we identified and selected 86 different categories in taking into account only ones having at least 15 occurrences. This decision was taken to ensure an independence of statistical results even whether the image database is changed. These 86 categories are listed in Table 1 ordered by category's label and in Table 2 ordered by category's *id* .
- Lastly, we added missing annotations to entities of the considered categories, except for too small size entities or entities belonging to a category having a high frequency of already annotated entities in the image, such as "leaf", "window", "flower", etc. In this way, the statistical results should not be biased by these missing annotations.

In the rest of the paper, we call DB this database. Now, we can ensure that the set of entities annotated in DB contains all the interesting entities that attract human attention view. Thus, this new annotated image database has a higher quality than the original one. Before beginning this work, we formulate two different hypotheses :

- The set of entities annotated in DB contains all the interesting objects that the photographer

2. Our website : <http://www.lamsade.dauphine.fr/~hoang/www/cartography>.

wants to present.

- The entities annotated are the ones attracting most attention view of LabelMe’s annotators, and contain a subset of interesting objects that the photographer wants to present.

Sometimes, the viewpoint of a photographer is different from public’s one. That means the subject annotated can be different from the photographer’s intention. Consequently, the statistical results would depend on annotations of LabelMe’s users. With the original database, the second hypothesis can represents a useful dataset for a study on human attention view. After a verification and a consolidation, we think that first hypothesis is verified with DB.



FIGURE 1 – Images of DB.

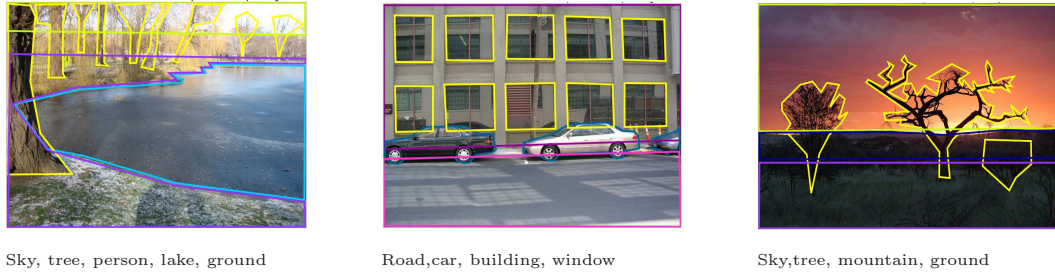


FIGURE 2 – Images of DB with their polygons and associated annotations.

2.2 Statistics on categories

Before studying different relationships between categories, we take a look at statistics concerning each category, for example, its highest and lowest numbers of entities in an image, the total number of its entities in DB, the number of images where at less one of its entities appears, etc. This statistical study is presented in Table 3. A overview of these statistics is presented in Table 4.

| Category label | Category ID | Category label | Category ID | Category label | Category ID |
|------------------|-------------|----------------|-------------|----------------|-------------|
| air conditioning | 21 | fire-hydrant | 46 | pot | 40 |
| arm | 65 | flag | 47 | railing | 28 |
| attic | 73 | flower | 55 | road | 09 |
| awning | 60 | grass | 43 | rock | 22 |
| balcony | 44 | grille | 29 | roof | 14 |
| bench | 48 | ground | 17 | sand | 69 |
| bicycle | 58 | handrail | 31 | sculpture | 81 |
| billboard | 78 | hat | 86 | sea | 71 |
| bird | 76 | head | 63 | sidewalk | 06 |
| blind | 27 | headlight | 30 | sign | 12 |
| block | 82 | lake | 74 | sky | 10 |
| boat | 70 | lamp | 33 | stair | 24 |
| box | 41 | leaf | 83 | street-light | 16 |
| building | 05 | license plate | 07 | table | 67 |
| bus | 61 | light | 39 | tail light | 19 |
| car | 02 | mailbox | 54 | text | 49 |
| chair | 50 | manhole | 23 | torso | 64 |
| chimney | 08 | mast | 79 | traffic light | 53 |
| clock | 62 | mirror | 18 | tree | 04 |
| cloud | 80 | motorbike | 77 | truck | 38 |
| column | 34 | mountain | 84 | umbrella | 68 |
| cone | 66 | pane | 35 | van | 37 |
| crosswalk | 59 | parking-meter | 51 | wall | 11 |
| curb | 52 | path | 56 | water | 72 |
| door | 25 | person | 36 | wheel | 26 |
| duck | 75 | pipe | 42 | window | 01 |
| fence | 03 | plant | 13 | wind-shield | 32 |
| field | 85 | pole | 15 | wire | 20 |
| fire escape | 45 | poster | 57 | | |

TABLE 1 – 86 entity categories in DB, ordered by label.

From Table 3, we can see that the average entities number of each category in an image could be used to have a quick view about the possibility of having more than one of its entities in an image. For example, category 1 (WINDOW) has a high number of occurrences in DB and its average is around 19 entities per image. That means that, if we find a WINDOW in an image, we can expect to find another WINDOW in the same image. Category 82 (BLOCK) has a considerable average also, around 10.25 entities per image. Meanwhile, some categories, like LAKE or SUN, do not have more than one entity per image. Certainly, it is not current to have two entities of LAKE in an image, and it is evident that there is only one SUN in the sky. Note that, because of a low number of occurrences of SUN in DB, we did not take into account this category in DB.

Interpretation with averages can provide quickly a general information on categories, but we can do it better. For a more detailed study, we have computed the intra-class correlation of categories, based on the classic correlation function between two categories. For a category, the inter-class correlation

| Category label | Category ID | Category label | Category ID | Category label | Category ID |
|------------------|-------------|----------------|-------------|----------------|-------------|
| window | 01 | headlight | 30 | crosswalk | 59 |
| car | 02 | handrail | 31 | awning | 60 |
| fence | 03 | wind-shield | 32 | bus | 61 |
| tree | 04 | lamp | 33 | clock | 62 |
| building | 05 | column | 34 | head | 63 |
| sidewalk | 06 | pane | 35 | torso | 64 |
| license plate | 07 | person | 36 | arm | 65 |
| chimney | 08 | van | 37 | cone | 66 |
| road | 09 | truck | 38 | table | 67 |
| sky | 10 | light | 39 | umbrella | 68 |
| wall | 11 | pot | 40 | sand | 69 |
| sign | 12 | box | 41 | boat | 70 |
| plant | 13 | pipe | 42 | sea | 71 |
| roof | 14 | grass | 43 | water | 72 |
| pole | 15 | balcony | 44 | attic | 73 |
| street-light | 16 | fire escape | 45 | lake | 74 |
| ground | 17 | fire-hydrant | 46 | duck | 75 |
| mirror | 18 | flag | 47 | bird | 76 |
| tail light | 19 | bench | 48 | motorbike | 77 |
| wire | 20 | text | 49 | billboard | 78 |
| air conditioning | 21 | chair | 50 | mast | 79 |
| rock | 22 | parking-meter | 51 | cloud | 80 |
| manhole | 23 | curb | 52 | sculpture | 81 |
| stair | 24 | traffic light | 53 | block | 82 |
| door | 25 | mailbox | 54 | leaf | 83 |
| wheel | 26 | flower | 55 | mountain | 84 |
| blind | 27 | path | 56 | field | 85 |
| railing | 28 | poster | 57 | hat | 86 |
| grille | 29 | bicycle | 58 | | |

TABLE 2 – 86 entity categories in DB, ordered by *id*.

function is defined as :

$$cor(x, y) = \frac{\sigma_{xy}}{\sigma_x \sigma_y} \quad (1)$$

$$= \frac{\sum_{i=1}^N (x_i - \bar{x}) \cdot (y_i - \bar{y})}{\sqrt{\sum_{i=1}^N (x_i - \bar{x})^2} \cdot \sqrt{\sum_{i=1}^N (y_i - \bar{y})^2}} \quad (2)$$

N is the number of images in DB. For a category C_j , every first entity found in an image is considered as variable x , another entity as variable y . Therefore, \bar{x} and \bar{y} are their average occurrence number in DB. In image I_i , if there is only one entity of C_j , then $x_i = 1$ and $y_i = 0$. If there are more than two entities, then $x_i = 1$ and $y_i = 1$. Otherwise, $x_i = 0$ and $y_i = 0$.

Slightly differently to classic correlation between two categories that represents impact of one cate-

| Categ. ID | Highest nb of occ. in an img | Average | Nb of occ. in all DB | Num of img. where categ. presents | Categ. ID | Highest nb of occ. in an img | Average | NB of occ. in all DB | Num of img. where categ. presents |
|--------------|---------------------------------------|---------|----------------------------|---|--------------|---------------------------------------|---------|----------------------------|---|
| 01 | 177 | 19.64 | 13297 | 677 | 02 | 31 | 4.59 | 2382 | 519 |
| 36 | 75 | 4.65 | 2295 | 494 | 05 | 32 | 2.75 | 2145 | 780 |
| 04 | 21 | 2.79 | 1758 | 630 | 26 | 13 | 4.03 | 1462 | 363 |
| 06 | 6 | 1.83 | 1123 | 614 | 12 | 11 | 2.28 | 964 | 423 |
| 25 | 8 | 2.04 | 822 | 403 | 10 | 4 | 1.11 | 821 | 740 |
| 09 | 4 | 1.16 | 744 | 641 | 13 | 8 | 1.81 | 615 | 340 |
| 16 | 11 | 1.7 | 564 | 331 | 27 | 45 | 7.31 | 446 | 61 |
| 15 | 17 | 1.92 | 435 | 226 | 65 | 26 | 4.05 | 421 | 104 |
| 44 | 24 | 3.41 | 395 | 116 | 07 | 4 | 1.42 | 352 | 248 |
| 32 | 5 | 1.67 | 345 | 206 | 30 | 8 | 1.82 | 298 | 164 |
| 18 | 4 | 1.42 | 295 | 208 | 64 | 20 | 2.89 | 292 | 101 |
| 63 | 18 | 2.67 | 288 | 108 | 19 | 6 | 1.71 | 286 | 167 |
| 60 | 12 | 2.23 | 252 | 113 | 49 | 6 | 1.62 | 248 | 153 |
| 43 | 5 | 1.5 | 246 | 164 | 58 | 7 | 1.83 | 218 | 119 |
| 34 | 20 | 3.1 | 214 | 69 | 11 | 4 | 1.36 | 202 | 149 |
| 35 | 14 | 3.1 | 195 | 63 | 03 | 5 | 1.43 | 192 | 134 |
| 53 | 5 | 1.87 | 189 | 101 | 24 | 5 | 1.34 | 155 | 116 |
| 21 | 11 | 1.8 | 142 | 79 | 33 | 12 | 2.22 | 140 | 63 |
| 28 | 7 | 1.73 | 126 | 73 | 31 | 7 | 1.97 | 124 | 63 |
| 23 | 5 | 1.4 | 120 | 86 | 55 | 5 | 1.52 | 111 | 73 |
| 51 | 4 | 1.42 | 109 | 77 | 84 | 5 | 1.39 | 106 | 76 |
| 29 | 9 | 2.43 | 102 | 42 | 47 | 6 | 1.63 | 96 | 59 |
| 70 | 18 | 3.67 | 88 | 24 | 17 | 3 | 1.14 | 82 | 72 |
| 57 | 10 | 1.88 | 75 | 40 | 76 | 11 | 1.4 | 73 | 52 |
| 14 | 5 | 1.43 | 73 | 51 | 40 | 4 | 1.61 | 71 | 44 |
| 73 | 19 | 3.33 | 70 | 21 | 48 | 5 | 1.79 | 68 | 38 |
| 83 | 9 | 2.16 | 67 | 31 | 56 | 3 | 1.16 | 67 | 58 |
| 37 | 5 | 1.26 | 67 | 53 | 22 | 14 | 2.78 | 64 | 23 |
| 59 | 3 | 1.17 | 61 | 52 | 50 | 18 | 3.05 | 61 | 20 |
| 08 | 3 | 1.33 | 60 | 45 | 38 | 3 | 1.26 | 58 | 46 |
| 72 | 2 | 1.08 | 55 | 51 | 46 | 3 | 1.07 | 48 | 45 |
| 42 | 5 | 1.31 | 46 | 35 | 68 | 7 | 2.15 | 43 | 20 |
| 82 | 20 | 10.25 | 41 | 4 | 52 | 3 | 1.21 | 41 | 34 |
| 75 | 9 | 3 | 36 | 12 | 71 | 3 | 1.06 | 35 | 33 |
| 67 | 15 | 2.33 | 35 | 15 | 54 | 4 | 1.4 | 35 | 25 |
| 61 | 3 | 1.13 | 34 | 30 | 39 | 5 | 2.06 | 33 | 16 |
| 86 | 32 | 32 | 32 | 1 | 80 | 5 | 1.52 | 32 | 21 |
| 78 | 5 | 1.36 | 30 | 22 | 69 | 2 | 1.17 | 28 | 24 |
| 41 | 4 | 1.22 | 28 | 23 | 81 | 10 | 1.93 | 27 | 14 |
| 20 | 7 | 2.45 | 27 | 11 | 85 | 3 | 1.44 | 26 | 18 |
| 66 | 4 | 1.47 | 25 | 17 | 62 | 2 | 1.05 | 23 | 22 |
| 79 | 4 | 1.57 | 22 | 14 | 77 | 3 | 1.31 | 21 | 16 |
| 45 | 4 | 1.9 | 19 | 10 | 74 | 1 | 1 | 16 | 16 |

TABLE 3 – Categories’ statistics in DB.

gory’s appearance on another, the intra-class correlation is never negative. Returning to the previous examples, we obtained 0.776 for the intra-class correlation of WINDOWS, that is also the highest score among intra-class correlations obtained. This score is high enough to conclude that we can find mostly at least twoWINDOWS in an image where a WINDOWS entity has already detected. The lowest score

| Nb of img/DB | Nb of entities/DB | Average of entities/cat.(STDEV) | Average of entities/img (STDEV) | Max. nb of entities/img | Min. nb of entities/img |
|-----------------|----------------------|------------------------------------|------------------------------------|----------------------------|----------------------------|
| 1133 | 38075 | 442.7 (1485.6) | 33.6 (32.3) | 264 | 1 |

TABLE 4 – Statistical overview of DB.

in this study is 0, related to LAKE category. Therefore, no image in DB contains more than a LAKE. In fact, it is not usual to have two or more instances of LAKE in the same image. Summarizing, 21 categories have intra-class correlation higher than 0.3 while only 8 categories have a score higher than 0.5, for example CAR, WINDOW, BUILDING (view histograms of inter-class correlation in Fig.3 and for more details, view Tab.16 in Annex A.1).

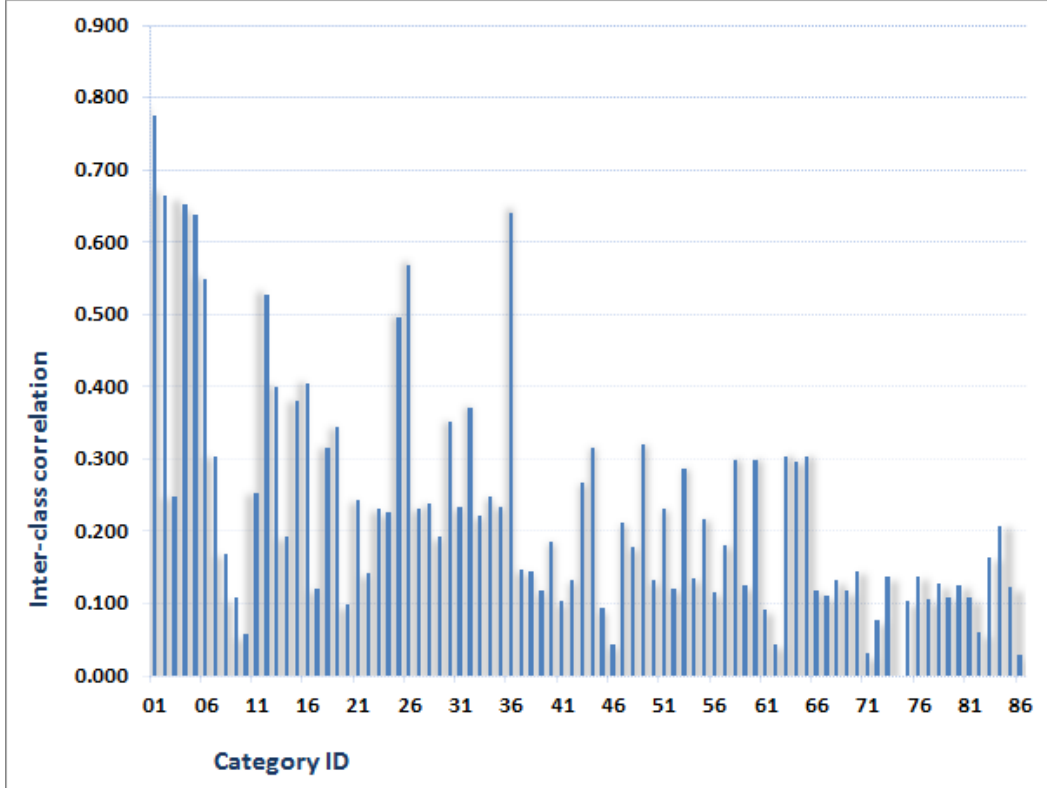


FIGURE 3 – Histogram of inter-class correlation of categories in DB.




This study can provide useful information in the category detection process, if we want, for example, to detect all entities of a category C_i present in an image I . Knowing that C_i has, in general, one entity per image (based on a threshold on correlation, for example), as soon as the first entity of C_i is detected, we could finish the detection process, thus reducing significantly the execution time of the detection. The statistics for all categories are available on our website².

In the next sections, we present a discuss of the statistical results on three different types of relationships : unary, binary and ternary relationships.

3 Unary relationships

3.1 Representation

We call unary relationship, the relationship between an entity and its localization in an image, where localization is defined as a region or area of the image, represented in this work by a code. More formally, let $A = \{A_i\}$, $I = \{I_j\}$, and $C = \{C_k\}$ be the set of areas, the set of images, and the set of categories, respectively. The unary relationship is an application R from $C \times I$ to A . $R(C_k, I_j) \in A$ allows knowing where C_k is located in I_j .

Areas of an image can be represented in different ways like quad-tree or quin-tree, see for example [11, 13]. Since we do not have any knowledge a priori of the location of the categories in the images, we propose to split images in a fixed number of regular areas (i.e. equal size areas). First, we divide each image in a fixed sized grid. Each cell of this grid, called atomic area, is represented by a code. Fig.4 and 5 depict a splitting in 9 or in 16 different basic areas and theirs codes, respectively. We then combine these codes to present more complex areas, by example for 9-area splitting, code 009 represents area  grouping together areas 001() and 008()





| | | |
|-----|-----|-----|
| 001 | 008 | 064 |
| 002 | 016 | 128 |
| 004 | 032 | 256 |

FIGURE 4 – Codes in unary relationship by splitting an image in nine areas.

| | | | |
|-------|-------|-------|-------|
| 00001 | 00016 | 00256 | 04096 |
| 00002 | 00032 | 00512 | 08192 |
| 00004 | 00064 | 01024 | 16384 |
| 00008 | 00128 | 02048 | 32768 |

FIGURE 5 – Codes in unary relationship by splitting an image in 16 areas.

3.2 Results analysis

The combination of nine 9-area splitting codes (Fig.4) gives 511 possible atomic/complex area codes. However, some codes could not be used, for example, code 017 () or code 161 () because their atomic areas are not connected by an edge (i.e. they are disjoint). It is impossible to have locations occupied by an entity in this way. In consequence, based on this idea, there are only 218 theoretically authorized codes (see the recursive algorithm to create theoretically authorized codes from a set of atomic codes in equation 16 of Annex B.1). Concretely, in DB, we did not find any entity in areas represented by impossible codes. Moreover, there are only 138 useful theoretically authorized codes, meaning that 80 codes are not encountered in DB. For example, DB does not contain any entity in areas with codes 47() or 125 (). In the same way, the combination of 16 codes in Fig.5 gives us 65535 different codes. In theory, we can reach 11506 atomic/complex areas (based on connected areas), but in DB, only 649 codes are present.

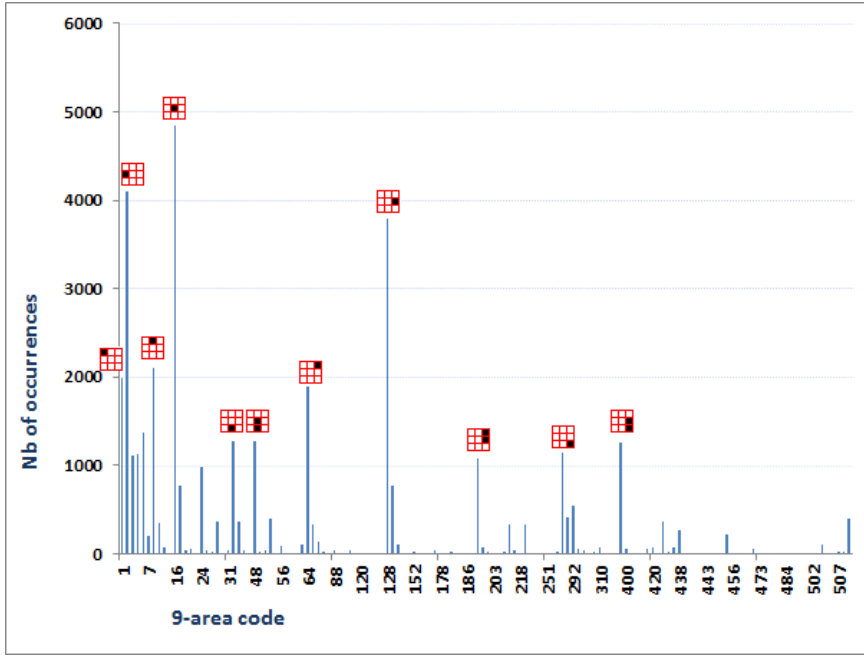


FIGURE 6 – Distribution of 9-area splitting codes.

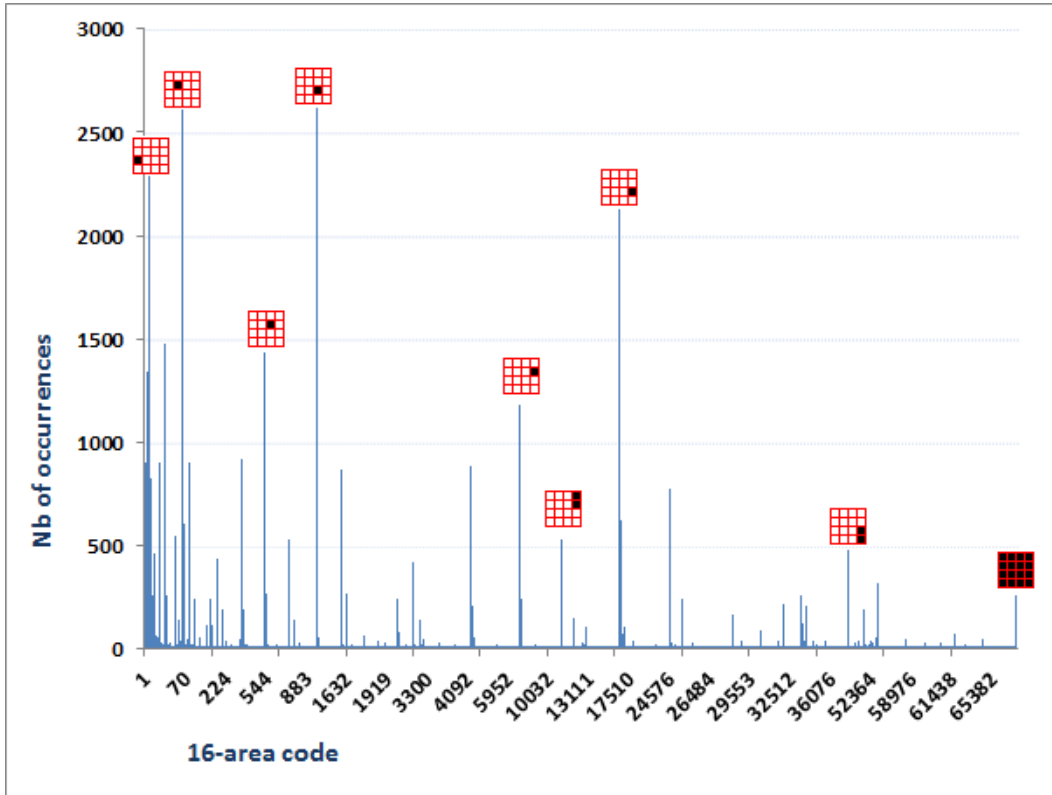


FIGURE 7 – Distribution of 16-area splitting codes.

An overview on present codes in DB for each type of splitting is represented in Fig.6 and 7.

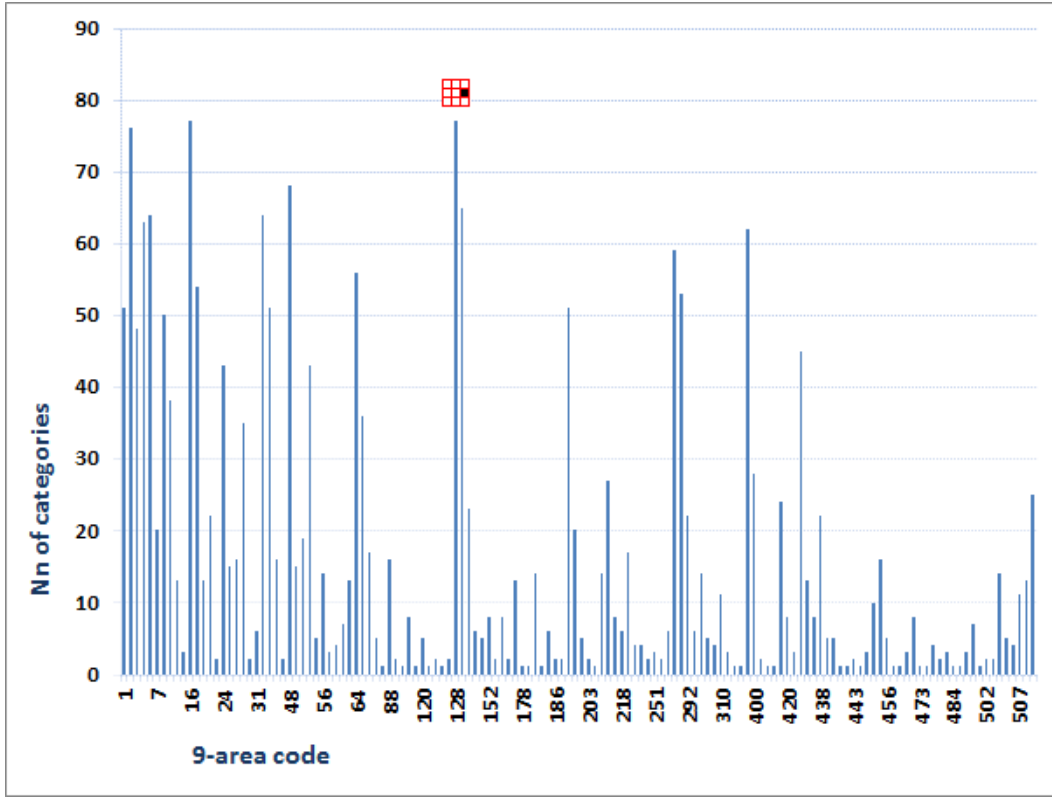


FIGURE 8 – Number of categories according to 9-area splitting codes.

For each type of splitting, we could retrieve easily number of occurrence or distribution of categories by report of their codes (view Fig.6 and 8 for 9-area splitting, Fig.7 and 9 for 16-area splitting). Some codes having the highest or lowest number of occurrences are reported in Table 5. In Annex B.1, Fig. 34 and 33 illustrate the distribution of categories according to two 9-area codes : 16(▣) (code having highest frequency) and 128(▣) (code concerning the most number of categories). Fig.36 and 35 represent a such distribution in 16-area splitting for codes 1024(▣) and 16384(▣). These informations provided us some interesting information to interpret the trend of categories' location in image.

3.3 Interpretation

From the Fig.6 and 7, we can observe that on the one hand, that large or complex regions have a small number of occurrences. That means that object categories are mostly represented by a simple and small area. On the other hand, the trend of the categories' presence, in first, is on the middle line, then, on the second line, and finally on a combination of the second and the third lines. In fact, it is not usual to present an interesting object only on the bottom line. And in practice, this line does not attract also the attention view. Similarly, we can observe that the trend of the categories' presence, on the left is higher than on the right. These conclusions confirm the well known rules concerning photography and ergonomics (human-computer interaction) :

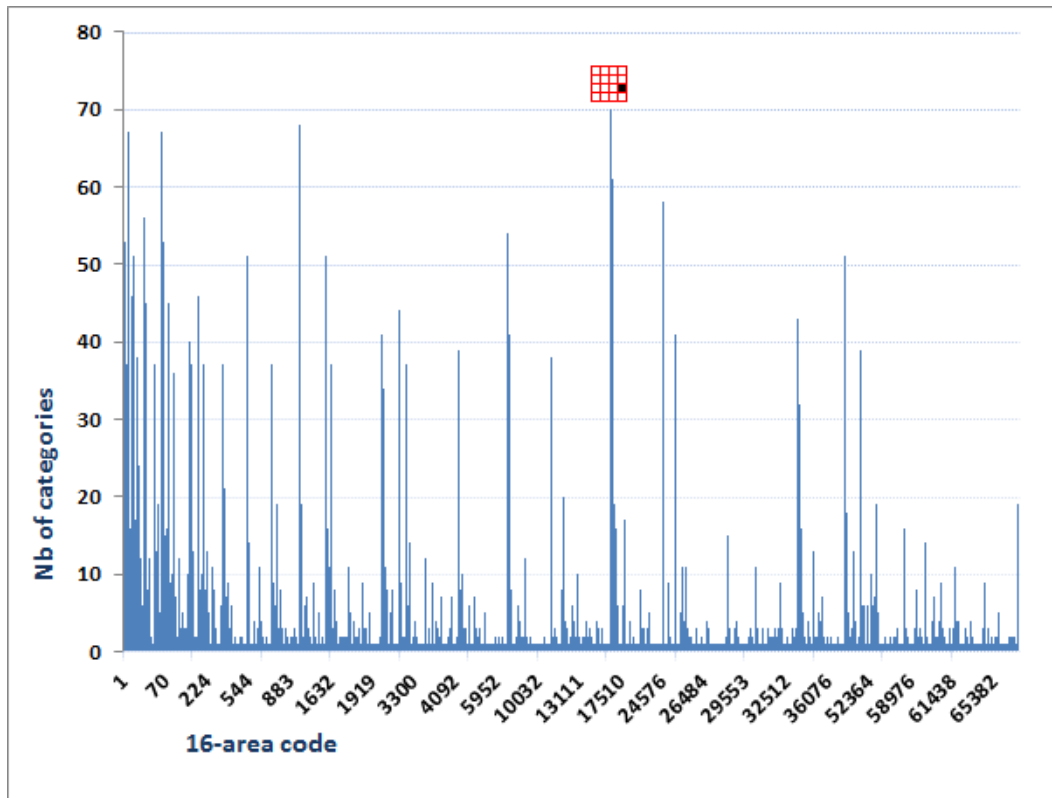


FIGURE 9 – Number of categories according to 16-area splitting codes.

- In photography, there is the rule of thirds³, one of the first rules of composition taught to most photography students. An image is cut by two horizontal lines and two vertical lines. It is recommended to present interesting object in the intersections or along the lines presented in this rule (see Fig.10).

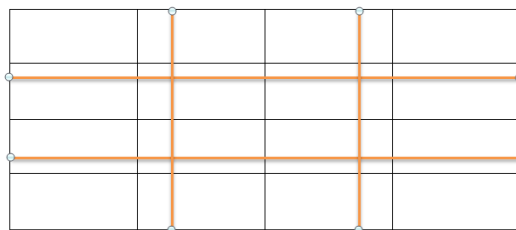










































FIGURE 10 – Horizontal and vertical lines in rule of thirds in photography.









































- According to [8, 10] concerning ergonomic studies on human-computer interaction, the center of computer screen is the most attracting. Next, the human attention view is attracted by the top and the left of screen more than by the bottom and the right consecutively, leading to slightly more annotated entities in these areas.

We have studied the distribution of categories across areas of the image, according to 9-area and 16-area splittings. Basically, the results obtained can be encapsulated in a knowledge-based system

3. <http://www.digital-photography-school.com/rule-of-thirds>

| | 20 codes having highest number of occurrence | | 20 codes having lowest number of occurrence | |
|----|---|------------|---|------------|
| | code | Nb of occ. | code | Nb of occ. |
| 1 |  | 4847 |  | 2 |
| 2 |  | 4091 |  | 2 |
| 3 |  | 3793 |  | 2 |
| 4 |  | 2100 |  | 1 |
| 5 |  | 1985 |  | 1 |
| 6 |  | 1889 |  | 1 |
| 7 |  | 1377 |  | 1 |
| 8 |  | 1277 |  | 1 |
| 9 |  | 1277 |  | 1 |
| 10 |  | 1266 |  | 1 |
| 11 |  | 1141 |  | 1 |
| 12 |  | 1130 |  | 1 |
| 13 |  | 1106 |  | 1 |
| 14 |  | 1073 |  | 1 |
| 15 |  | 987 |  | 1 |
| 16 |  | 772 |  | 1 |
| 17 |  | 766 |  | 1 |
| 18 |  | 540 |  | 1 |
| 19 |  | 410 |  | 1 |
| 20 |  | 404 |  | 1 |

(a) 40 codes in 9-area splitting having highest and lowest number of occurrences.

| | 20 codes having highest number of occurrence | | 20 codes having lowest number of occurrence | |
|----|---|------------|---|------------|
| | code | Nb of occ. | code | Nb of occ. |
| 1 |  | 2618 |  | 1 |
| 2 |  | 2613 |  | 1 |
| 3 |  | 2288 |  | 1 |
| 4 |  | 2126 |  | 1 |
| 5 |  | 1479 |  | 1 |
| 6 |  | 1430 |  | 1 |
| 7 |  | 1343 |  | 1 |
| 8 |  | 1183 |  | 1 |
| 9 |  | 919 |  | 1 |
| 10 |  | 904 |  | 1 |
| 11 |  | 903 |  | 1 |
| 12 |  | 900 |  | 1 |
| 13 |  | 883 |  | 1 |
| 14 |  | 869 |  | 1 |
| 15 |  | 823 |  | 1 |
| 16 |  | 777 |  | 1 |
| 17 |  | 618 |  | 1 |
| 18 |  | 609 |  | 1 |
| 19 |  | 605 |  | 1 |
| 20 |  | 550 |  | 1 |

(b) 40 codes in 16-area splitting having highest and lowest number of occurrences. There are 223 codes present only one time in DB.

TABLE 5 – 40 codes having highest and lowest number of occurrences of each type of splitting.

where they will be interpreted as a probability of presence of a given category in a given area. For example with 9-area splitting, CHIMNEY and SKY appear more frequently on the top of the image, with probabilities 0.72 and 0.81 respectively ; see them respective distribution in Fig. 11 and 12. In a object detection task for example, these measures can help in determining priority searching areas, and then in reducing the searching space of the objects. They are available for all categories on our website².

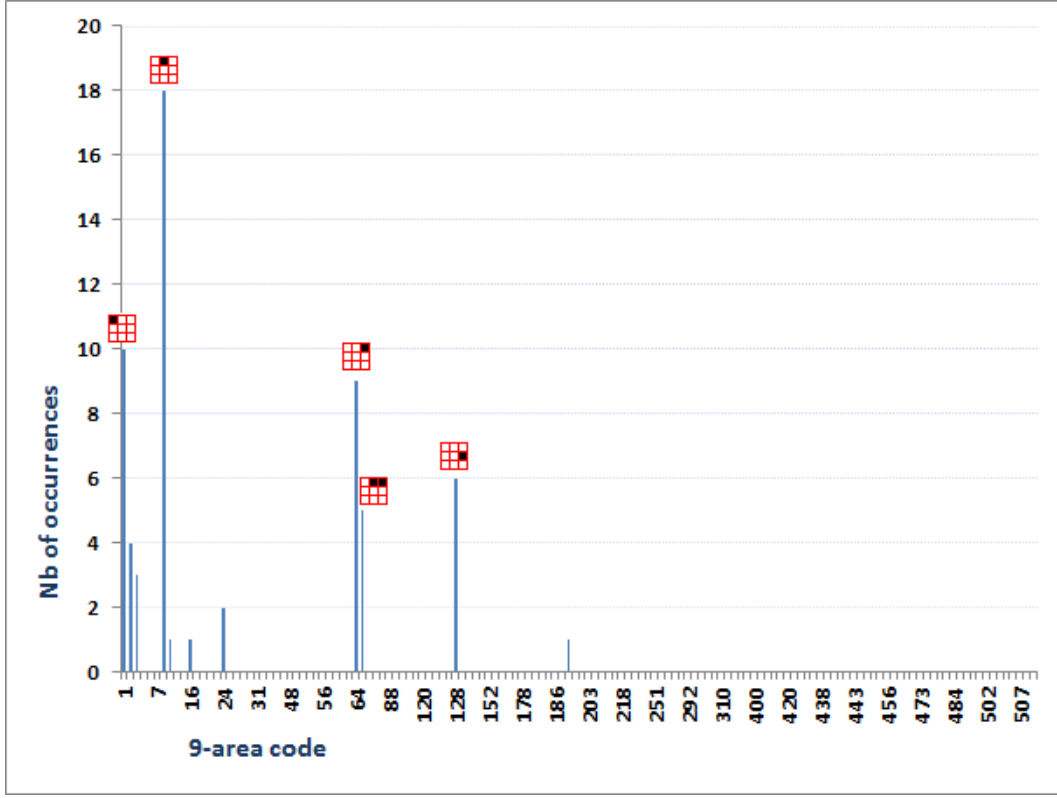


FIGURE 11 – Appearance of CHIMNEY in DB with 9-area splitting.

3.4 Spatial reasoning

We have also a question : "*Could a category be frequently and entirely present in a given area ?*". This question could help us to find an efficient method for detecting a category in an image. This idea drives us to examine the distribution of occurrences of each category C_j according to each theoretically possible area in the image, by the way of a normalized histogram : $H_{split}(C_j)$ with $split \in \{9\text{-area}, 16\text{-area}\}$.

When a category is integrally in an area A_i of $split$, it can probably appear in a smaller theoretically authorized area A_k included in A_i . Let FC be the function allowing to create theoretically possible areas from A_i (see Equa. 16 in Annex B.1). $\{A_k\} = FC_{split}(A_i)$. Let $SC_{split}(A_i)$ be the set of codes of every theoretically authorized areas A_k in A_i :

$$SC_{split}(A_i) = \{cod(A_k) | A_k \in FC_{split}(\{A_{split}\})\} \quad (3)$$

where $cod(A_k)$ is the code representing area A_k . A category C_j , whose instances appear entirely in A_i , has a specific histogram where the number of occurrences of a code c , $c \in SC_{split}(A_i)$, is not null. Then, to do spatial reasoning on such histograms, we propose a function FH such as :

$$FH(H_{split}(C_j), A_i) = G_{split} \odot H_{split}(C_j) \quad (4)$$

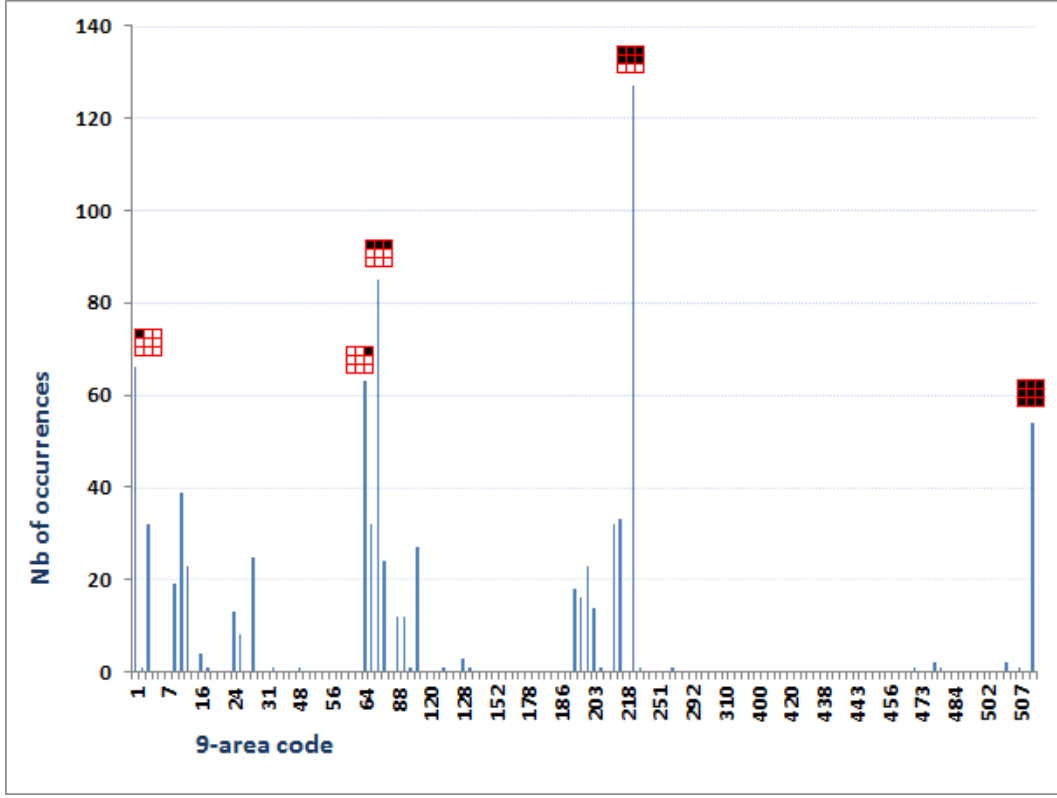





FIGURE 12 – Appearance of SKY in DB with 9-area splitting.

where \odot is the dot product and G a 1D template mask of size the number of theoretical codes c according to the splitting method :

$$G_{split}(c) = \begin{cases} 0 & \text{if } c \in SC_{split}(A_i) \\ 1 & \text{otherwise} \end{cases} \quad (5)$$

FH has values varying in $[0..1]$; $FH = 0$ means that all not null frequencies correspond to codes $SC_{split}(A_i)$, and then that category C_j is always entirely in area A_i . If $FH = 1$, we can say that C_j is never entirely in A_i . The more FH is high, the less C_j appears entirely in A_i . We present categories according to highest/smallest FH in Tab.6 for 9-area splitting and in Tab.7 for 16-area splitting. From FH , we can deduce the probability p_a of presence of C_j in A_i as $p_a(A_i) = 1 - FH$.

More generally, if we examine the presence of C_j in n disjoint areas A_i , the probability becomes $p_a(\{A_i\}_n) = \sum_{i=1}^n (1 - FH(H_{split}(C_j), A_i))$. For category PERSON for example, the values FH for the three A_i areas    in 9-area splitting are respectively 0.704, 0.644 and 0.721, that gives $p_a(\{A_i\}_3) = 0.931$. This result means that the probability of category PERSON to be entirely in one column is high, and that its presence in two columns at least is very small. Consequently, we can say that in DB, entities PERSON are present vertically most of the time, and that they appear rarely at scales larger than one column. These statistics can help designing a person detection task for future applications. Similar spatial reasoning can be done with other categories and other areas. For each category, it

| | | 1st line | | 2nd line | | 3rd line | |
|------------------|----------------|----------|----------|----------|-----------|----------|-----------|
| | | C_i | F | C_i | FH | C_i | FH |
| Horizontal lines | 10 smallest FH | 8 | 0.283 | 86 | 0.062 | 23 | 0.041 |
| | | 20 | 0.444 | 70 | 0.193 | 59 | 0.213 |
| | | 21 | 0.45 | 60 | 0.198 | 82 | 0.219 |
| | | 73 | 0.542 | 68 | 0.302 | 22 | 0.375 |
| | | 62 | 0.565 | 32 | 0.327 | 52 | 0.439 |
| | | 14 | 0.589 | 18 | 0.328 | 7 | 0.491 |
| | | 33 | 0.621 | 63 | 0.347 | 67 | 0.514 |
| | | 1 | 0.622 | 49 | 0.366 | 26 | 0.545 |
| | | 10 | 0.629 | 61 | 0.411 | 30 | 0.553 |
| | | 44 | 0.63 | 37 | 0.417 | 58 | 0.555 |
| | 10 highest FH | 71 | 1 | 82 | 0.926 | 20 | 0.999 |
| | | 66 | 1 | 17 | 0.926 | 62 | 0.999 |
| | | 59 | 1 | 69 | 0.928 | 73 | 0.999 |
| | | 54 | 1 | 74 | 0.937 | 79 | 0.999 |
| | | 52 | 1 | 9 | 0.939 | 42 | 0.999 |
| | | 46 | 1 | 23 | 0.975 | 86 | 1 |
| | | 40 | 1 | 42 | 0.978 | 21 | 1 |
| | | 65 | 1 | 10 | 0.987 | 80 | 1 |
| | | 64 | 1 | 20 | 0.999 | 8 | 1 |
| | | 23 | 1 | 59 | 1 | 74 | 1 |
| Vertical lines | 10 smallest FH | 79 | 0.59 | 82 | 0.365 | 39 | 0.515 |
| | | 42 | 0.608 | 54 | 0.371 | 22 | 0.578 |
| | | 46 | 0.625 | 27 | 0.52 | 47 | 0.583 |
| | | 48 | 0.632 | 19 | 0.524 | 66 | 0.6 |
| | | 34 | 0.635 | 45 | 0.526 | 38 | 0.637 |
| | | 77 | 0.666 | 75 | 0.527 | 46 | 0.645 |
| | | 29 | 0.666 | 86 | 0.531 | 62 | 0.652 |
| | | 51 | 0.669 | 81 | 0.555 | 15 | 0.653 |
| | | 68 | 0.674 | 33 | 0.557 | 29 | 0.656 |
| | | 16 | 0.687 | 41 | 0.571 | 73 | 0.657 |
| | 10 highest FH | 61 | 0.882 | 17 | 0.963 | 43 | 0.898 |
| | | 85 | 0.884 | 72 | 0.963 | 17 | 0.902 |
| | | 84 | 0.905 | 69 | 0.964 | 14 | 0.917 |
| | | 59 | 0.918 | 84 | 0.971 | 59 | 0.918 |
| | | 74 | 0.937 | 9 | 0.985 | 56 | 0.94 |
| | | 17 | 0.939 | 85 | 0.999 | 9 | 0.955 |
| | | 71 | 0.942 | 80 | 1 | 72 | 0.963 |
| | | 75 | 0.944 | 59 | 1 | 69 | 0.964 |
| | | 72 | 0.945 | 74 | 1 | 71 | 0.971 |
| | | 9 | 0.961 | 71 | 1 | 74 | 1 |

TABLE 6 – Ranking of categories according to particular location in 9-area splitting.

is possible to expose a study that can exhibit a specific size, shape and area(s) for a searching/detection process. For example, we examine the center area of images in DB with 16-area splitting. From Tab.8, we saw that there are five categories having frequency more than 50% : MIRROR, TAIL LIGHT (of car), HAT, MAILBOX, HEAD (of person). If we would like search these categories in images, we could begin the process by the center area.

| | | 1st line | | 2nd line | | 3rd line | | 4th line | |
|------------------|----------------|----------|-------|----------|-------|----------|-------|----------|-------|
| | | C_i | FH | C_i | FH | C_i | FH | C_i | FH |
| Horizontal lines | 10 smallest FH | 8 | 0.449 | 33 | 0.485 | 18 | 0.206 | 23 | 0.208 |
| | | 20 | 0.629 | 73 | 0.514 | 19 | 0.227 | 22 | 0.531 |
| | | 73 | 0.699 | 62 | 0.521 | 32 | 0.237 | 59 | 0.606 |
| | | 21 | 0.718 | 21 | 0.528 | 54 | 0.257 | 67 | 0.714 |
| | | 10 | 0.747 | 47 | 0.572 | 30 | 0.258 | 17 | 0.78 |
| | | 80 | 0.75 | 14 | 0.575 | 7 | 0.275 | 50 | 0.786 |
| | | 1 | 0.755 | 86 | 0.593 | 63 | 0.295 | 52 | 0.804 |
| | | 44 | 0.756 | 49 | 0.616 | 41 | 0.321 | 39 | 0.818 |
| | | 45 | 0.789 | 68 | 0.627 | 46 | 0.333 | 40 | 0.83 |
| | | 27 | 0.804 | 39 | 0.636 | 51 | 0.339 | 6 | 0.831 |
| | 10 highest FH | 71 | 1 | 77 | 1 | 44 | 0.967 | 79 | 0.999 |
| | | 66 | 1 | 72 | 1 | 83 | 0.97 | 86 | 1 |
| | | 54 | 1 | 82 | 1 | 76 | 0.972 | 74 | 1 |
| | | 51 | 1 | 71 | 1 | 42 | 0.978 | 44 | 1 |
| | | 46 | 1 | 66 | 1 | 8 | 0.983 | 80 | 1 |
| | | 23 | 1 | 54 | 1 | 14 | 0.986 | 75 | 1 |
| | | 65 | 1 | 23 | 1 | 10 | 0.996 | 38 | 1 |
| | | 64 | 1 | 17 | 1 | 20 | 0.999 | 27 | 1 |
| | | 59 | 1 | 59 | 1 | 79 | 0.999 | 8 | 1 |
| | | 52 | 1 | 52 | 1 | 80 | 1 | 10 | 1 |
| Vertical lines | 10 smallest FH | 42 | 0.717 | 54 | 0.6 | 82 | 0.609 | 39 | 0.575 |
| | | 51 | 0.724 | 82 | 0.658 | 81 | 0.629 | 66 | 0.64 |
| | | 79 | 0.727 | 41 | 0.678 | 47 | 0.656 | 22 | 0.703 |
| | | 21 | 0.753 | 66 | 0.68 | 33 | 0.657 | 29 | 0.725 |
| | | 40 | 0.76 | 27 | 0.683 | 75 | 0.666 | 47 | 0.729 |
| | | 77 | 0.761 | 45 | 0.684 | 21 | 0.683 | 46 | 0.729 |
| | | 34 | 0.771 | 19 | 0.685 | 86 | 0.687 | 62 | 0.739 |
| | | 16 | 0.774 | 34 | 0.696 | 62 | 0.695 | 15 | 0.743 |
| | | 53 | 0.777 | 46 | 0.708 | 51 | 0.697 | 41 | 0.749 |
| | | 60 | 0.781 | 18 | 0.708 | 27 | 0.697 | 78 | 0.766 |
| | 10 highest FH | 75 | 0.944 | 9 | 0.994 | 10 | 0.982 | 17 | 0.951 |
| | | 84 | 0.962 | 69 | 0.999 | 59 | 0.983 | 56 | 0.955 |
| | | 9 | 0.971 | 85 | 0.999 | 9 | 0.995 | 69 | 0.964 |
| | | 17 | 0.975 | 20 | 0.999 | 69 | 0.999 | 9 | 0.966 |
| | | 72 | 0.981 | 71 | 1 | 85 | 0.999 | 59 | 0.967 |
| | | 59 | 0.983 | 72 | 1 | 84 | 0.999 | 75 | 0.972 |
| | | 69 | 0.999 | 74 | 1 | 80 | 1 | 14 | 0.972 |
| | | 61 | 1 | 17 | 1 | 71 | 1 | 72 | 0.981 |
| | | 86 | 1 | 59 | 1 | 74 | 1 | 71 | 1 |
| | | 74 | 1 | 52 | 1 | 17 | 1 | 74 | 1 |

TABLE 7 – Ranking of categories according to particular location in 16-area splitting.

4 Binary relationships

A binary relationship links two entities of distinct categories together in an image. It can be a co-occurrence or a spatial relationship. From the 86 categories of the database used, there are 3655 possible binary relationships between categories. Among them, we observed first that 879 couples of categories never occur together. For more details, the reader can consult Fig.13 which present a map of co-occurrences categories and Fig.14 for a map showing absent couples. Before studying spatial binary

| | Border | | Center | |
|---------------|--------|-------|--------|-------|
| | C_i | FH | C_i | FH |
| 10 smallest F | 45 | 0.631 | 86 | 0.406 |
| | 8 | 0.65 | 19 | 0.447 |
| | 42 | 0.673 | 18 | 0.45 |
| | 21 | 0.697 | 54 | 0.457 |
| | 29 | 0.705 | 63 | 0.468 |
| | 51 | 0.706 | 82 | 0.512 |
| | 1 | 0.719 | 75 | 0.527 |
| | 66 | 0.72 | 25 | 0.54 |
| | 68 | 0.72 | 51 | 0.541 |
| | 79 | 0.727 | 65 | 0.541 |
| 10 highest F | 59 | 0.918 | 83 | 0.97 |
| | 69 | 0.928 | 84 | 0.971 |
| | 71 | 0.942 | 17 | 0.975 |
| | 75 | 0.944 | 59 | 0.983 |
| | 84 | 0.952 | 10 | 0.987 |
| | 9 | 0.961 | 9 | 0.987 |
| | 17 | 0.963 | 85 | 0.999 |
| | 72 | 0.981 | 20 | 0.999 |
| | 86 | 1 | 71 | 1 |
| | 74 | 1 | 74 | 1 |

TABLE 8 – Ranking of categories according to "border" and "center" locations in 16-area. splitting.

relationships, we examine co-occurrence relationships.

4.1 Co-occurrence relationships

To begin, we give an example. In DB, WINDOW appears in 677 images and CAR in 519 images. This couple of categories appears together in 480 images. Then, we can conclude that their co-occurrence relationship is quite remarkable : for instance, 92% of the images containing a CAR also contain a WINDOW. This rate corresponds to a conditional probability, denoted $P(\text{WINDOW}|\text{CAR})$. Fig.15 gives an idea of the distribution of the number of images where all the category couples appear. Couples having a high number of occurrences are listed in Tab.9. Additionally, we can compute their correlation to learn more about the co-occurrence of such couples. Hence, these measures can help understanding better which category's presence conducts to the presence or absence of another category. Statistics for some couples can be found in Tab. 9.

The correlation score resumes in one value the presence or absence together of two categories and especially the strength of this knowledge. We can apply the formula of equation 1. Variable x_i shows the presence of at least on instance of category C_j in an image I_i , then $x_i = 1$ if this condition is satisfied, otherwise $x_i = 0$. Variable y_i concerns another category C_k . Then \bar{x} and \bar{y} are their average occurrence number in database. Hence, if a couple's correlation is negative, then this couple is rarely present in a same image. The highest score obtained is 0.984 for TORSO-ARM ; in fact, only 3 couples have a correlation higher than 0.8 (the distribution of these correlation is displays in Fig.37 of Annex

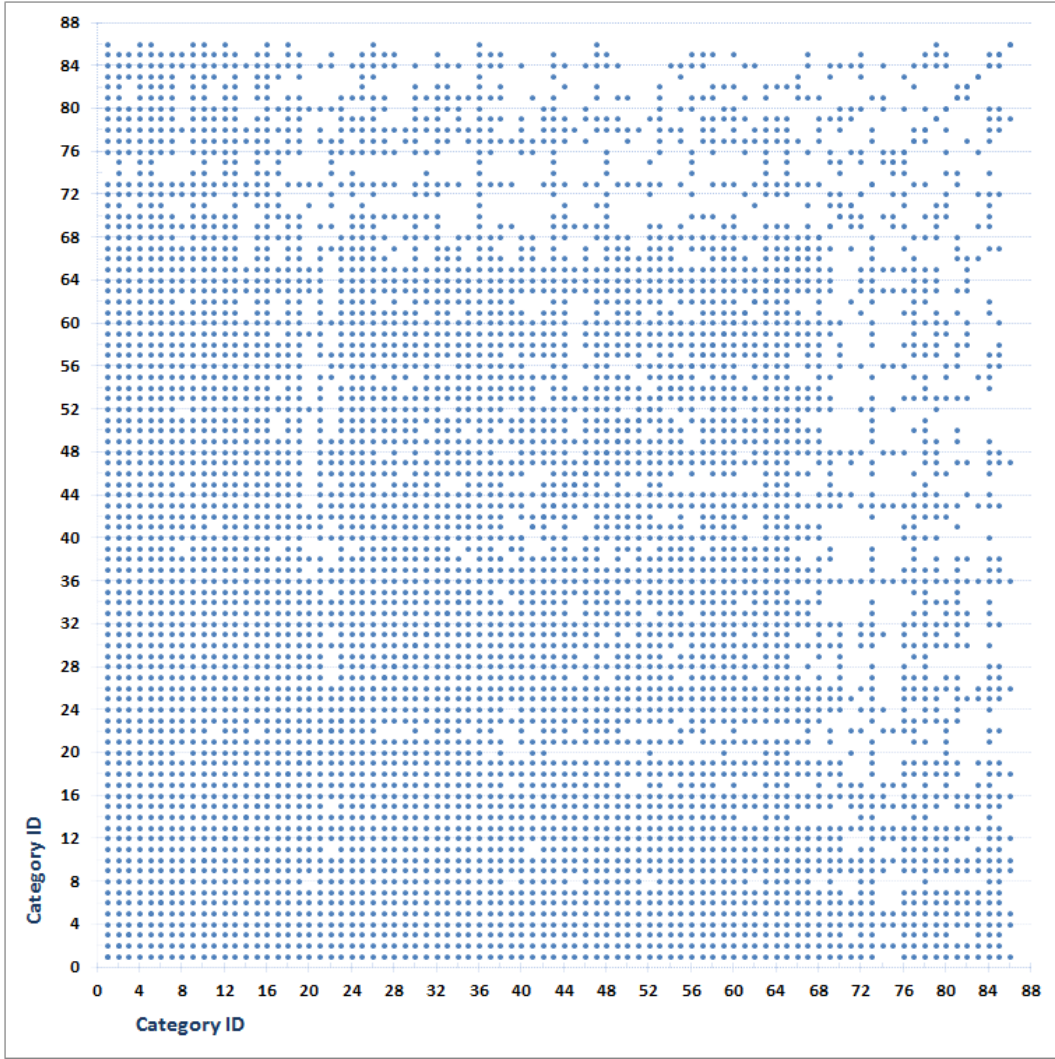


FIGURE 13 – Occurrence relationships between two categories in DB.

| Couples ($A - B$) | Nb of occur. of couples | $P(A)$ | $P(B)$ | $P(A \cap B)$ | $P(A B)$ | $P(B A)$ | Corr. |
|--------------------------|----------------------------|--------|--------|---------------|----------|----------|--------|
| window-car | 57925 | 0.598 | 0.458 | 0.424 | 0.925 | 0.709 | 0.609 |
| building-sidewalk | 3051 | 0.688 | 0.542 | 0.535 | 0.987 | 0.777 | 0.696 |
| window-building | 38173 | 0.598 | 0.688 | 0.591 | 0.859 | 0.990 | 0.788 |
| window-lake | 0 | 0.598 | 0.014 | 0.000 | 0.000 | 0.000 | -0.149 |
| car-tail light | 1591 | 0.458 | 0.147 | 0.147 | 1.000 | 0.321 | 0.450 |
| chimney-sky | 78 | 0.040 | 0.653 | 0.040 | 0.061 | 1.000 | 0.146 |
| building-bird | 15 | 0.688 | 0.046 | 0.004 | 0.077 | 0.005 | -0.297 |
| arm-torso | 2262 | 0.089 | 0.092 | 0.089 | 0.971 | 1.000 | 0.984 |

TABLE 9 – Couples of categories having either a highest number of occurrences or a highest conditional probability or a highest correlation.

C.1, some obvious scores can be found in Tab.18 of the same Annex). The lowest score obtained is -0.297 for couple BUILDING-BIRD (view Table 9). Hence, any couple in database has a strong decor-

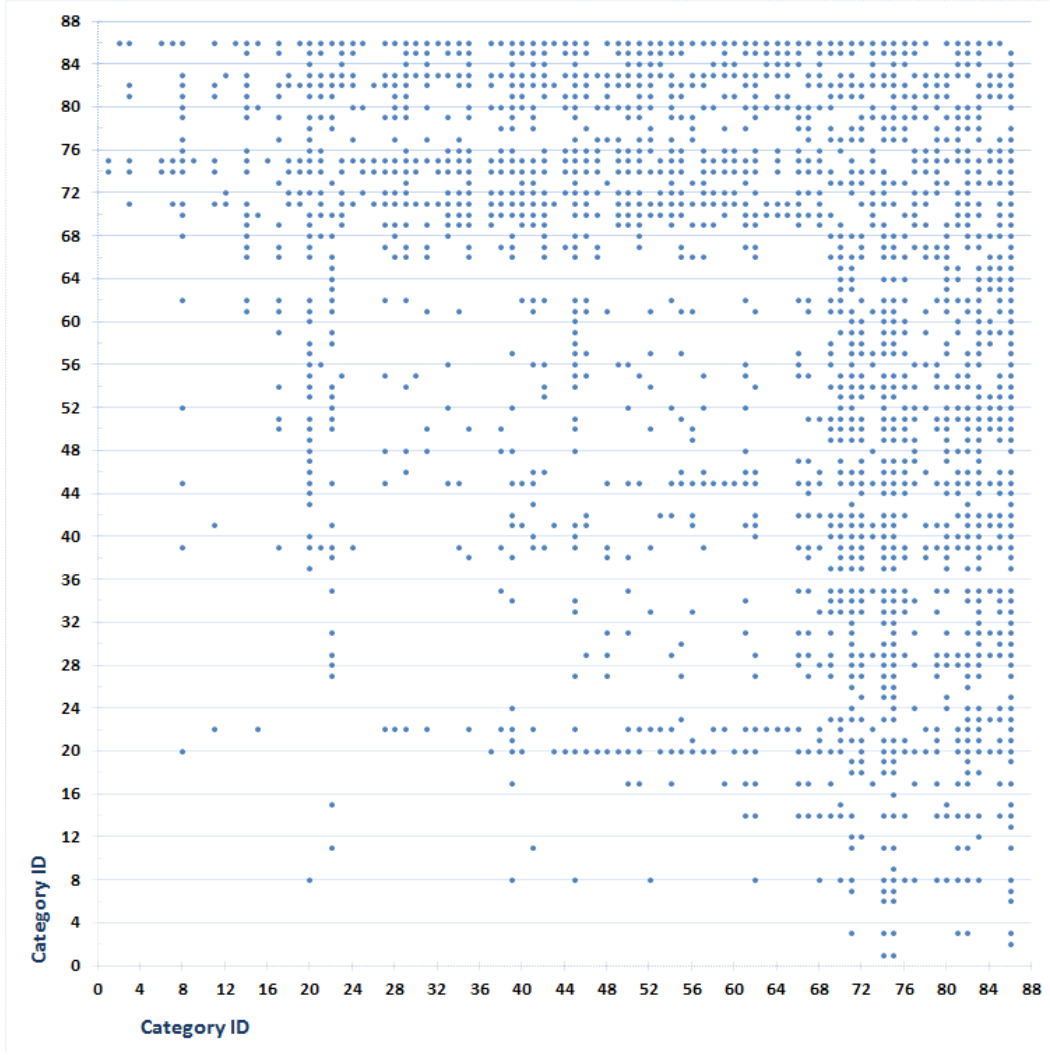


FIGURE 14 – Couples of two categories that do not appear jointly in images of DB.

relation state. These results cannot conduct to the conclusion on correlation or decorrelation of most of the couples of categories.

But conditional probabilities can help to go deeper in the analysis. The conditional probability is computed as $P(B | A) = \frac{P(A \cap B)}{P(A)}$. $P(A)$ and $P(B)$ is presence probability of A and B respectively. $P(A) = \frac{N_I(A)}{N_T}$ where $N_I(A)$ number of images where A appears and N_T number of images of DB. $P(A \cap B)$ is presence probability of the couple (A, B) . For example, $P(\text{BUILDING} | \text{SIDEWALK})$ is very high (see Table 9). That means that, in detecting a SIDEWALK, we can expect finding a BUILDING in the same image. Such relationship should be integrated with benefit in a knowledge-based system dedicated to artificial vision. Indeed, sidewalks are easy to detect because of their specific and universal visual appearance, while the variability of buildings makes them harder to detect. Then the prior detection of a sidewalk would contribute to facilitate the detection of a building by reducing the number of images to process. This reasoning can be generalized to other couples of categories, since in total, there are

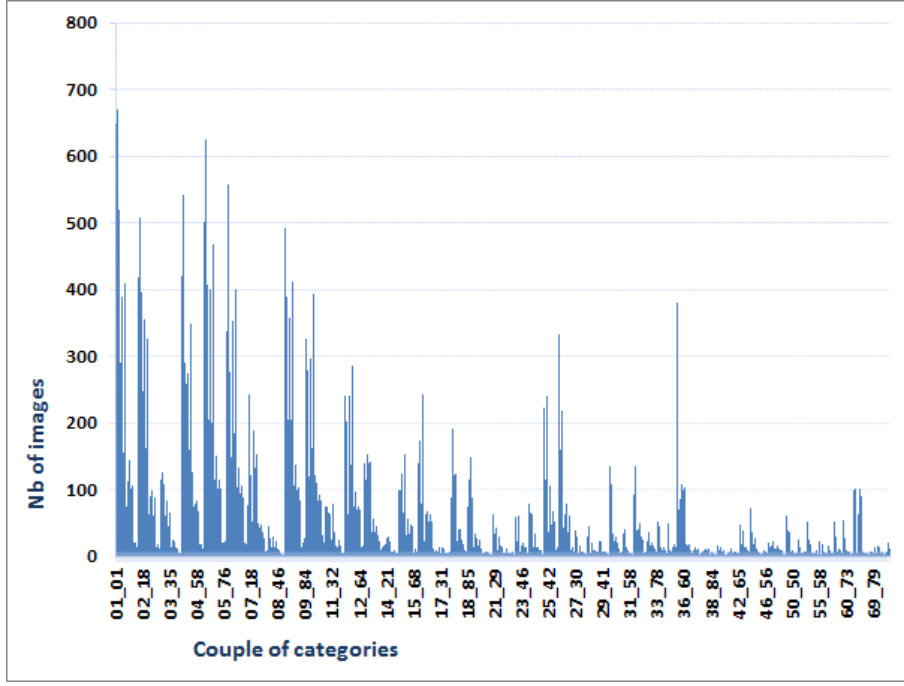


FIGURE 15 – Number of images where couples of categories appear in.

141 conditional probabilities higher than 0.95. Note that 66 of them are equal to 1 (see examples in Table 9), making the possibility of replacing the detection step of one category by the detection step of another, if easier, to find images of that category. All these measures are available on the website² of this work. Their distribution is displays in Fig.38 of Annex C.1.

4.2 Binary spatial relationship

In last years, there have been many approaches proposed for representing binary spatial relationships. They can be classified as topological, directional or distance-based approaches (see [4] for more details), and can be applied on symbolic objects or low level features. Here, we have focussed on relationships between the entities of the database described in terms of directional relationships with approach 9DSpa [7], of topological relationships [3] and of a combination of them with 2D projections [9]. We do not use orthogonal [2] and 9DLT relationship [1] because of its inconveniences mentioned in [7]. The detail of each approach is explained in the following sections.

4.2.1 9DSpa relationships

9DSpa describes directional relationships between a reference entity and another one based on the combination of 9 codes associated to areas orthogonally built around the MBR (Minimum Bounding Rectangle) of the reference entity. To complete this description, the autors take into account topological relationships. Because we want to study distinctly topological relationships, we examined only

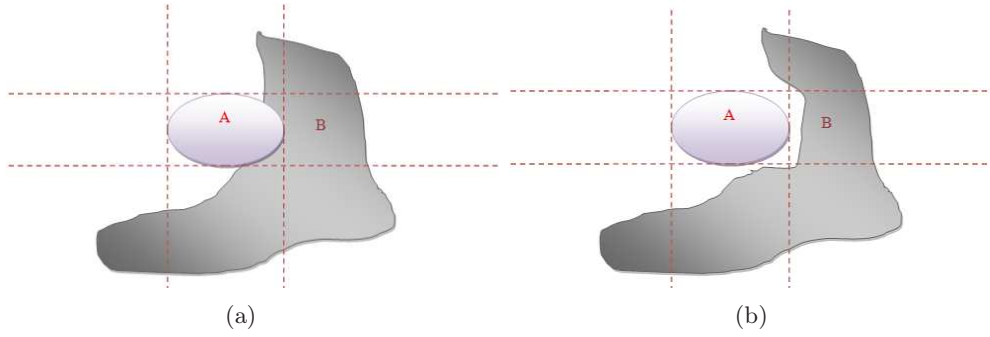


FIGURE 16 – Original 9DSpa coding gives the same code for these two cases : 11100111 = 231.

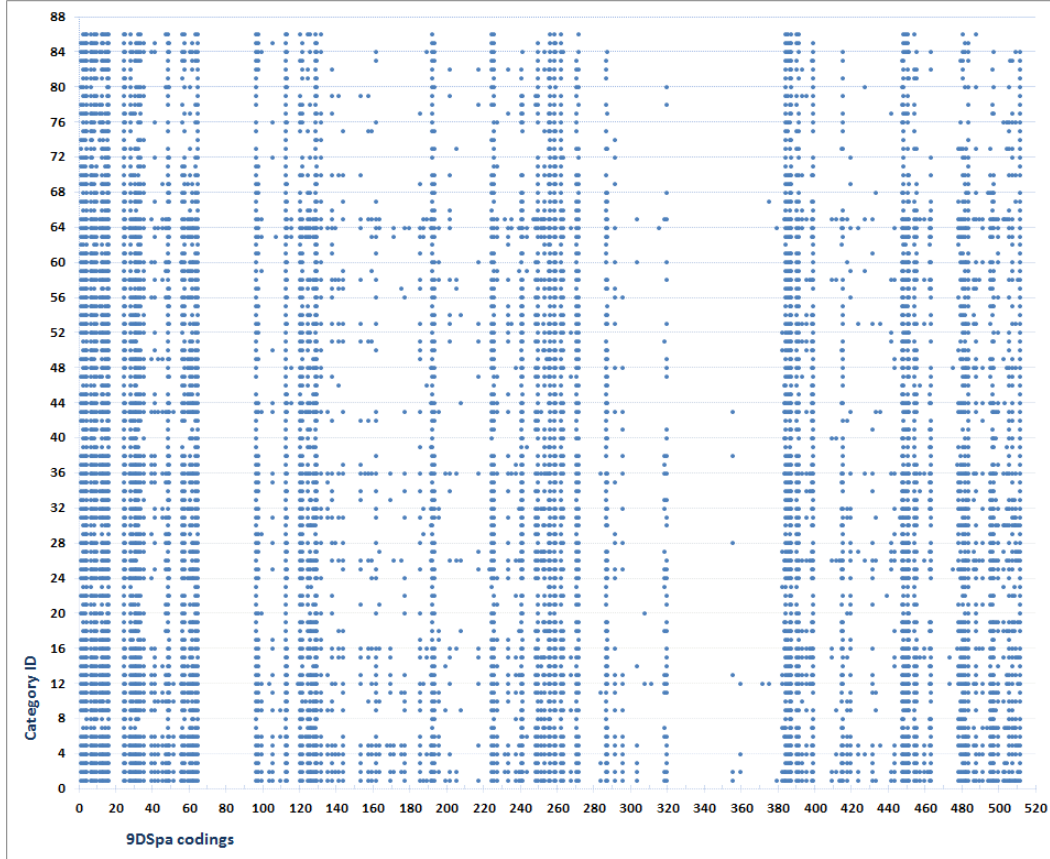


FIGURE 17 – Distribution of the 9DSpa codes for each category in DB.

the directional part of this approach. With the original 9DSpa approach, the description of the code uses only 8 bits, then, the center (or MBR of reference object) is coded by 0. With this type of code, we cannot identify if the second entity in a couple overlaps the MBR of reference one (see example in Figure 16). Therefore, we use a new description based on 9 bits to recognize the intersection between two entities (see Table 10).

Firstly, we present a overview of the 9DSpa codes that can be encountered for each category in Fig.17. 9DSpa approach gives 511 possible codes. But we saw that several codes are never used and

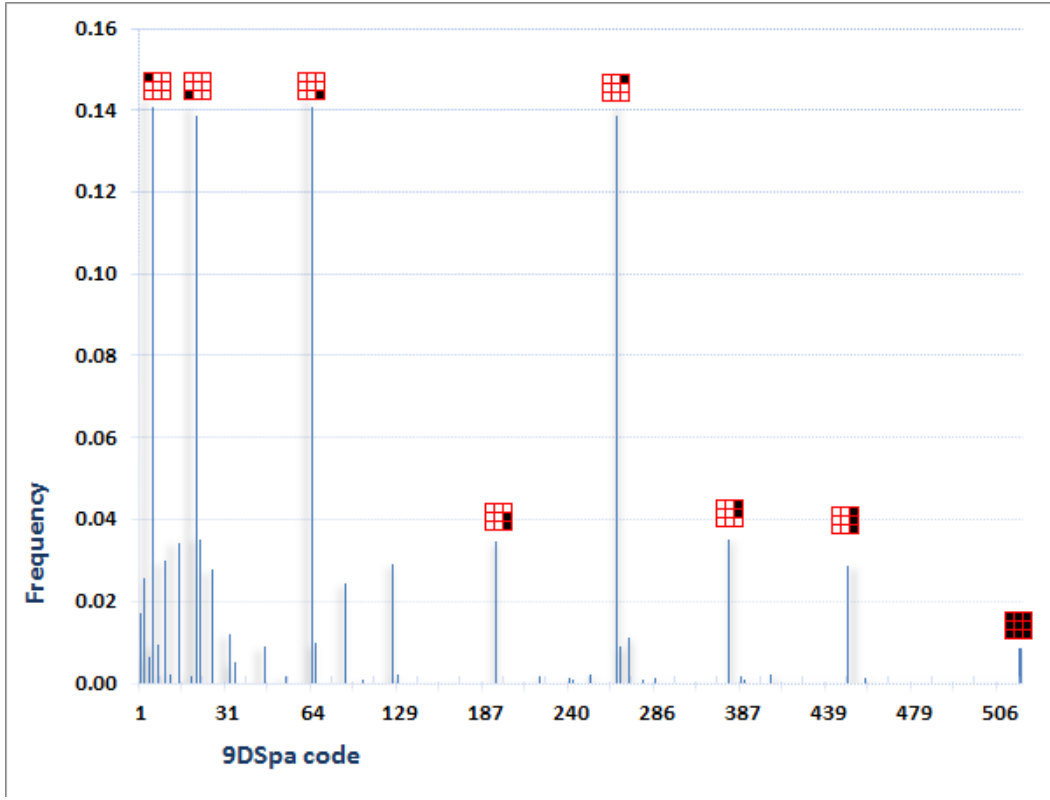


FIGURE 18 – Distribution of 9DSpa codes.

| | | |
|-----------------|-----------------|-----------------|
| 000000100 = 004 | 000000010 = 002 | 100000000 = 256 |
| 000001000 = 008 | 000000001 = 001 | 010000000 = 128 |
| 000010000 = 016 | 000100000 = 032 | 001000000 = 064 |

TABLE 10 – Modified codes in 9DSpa approach.

be not associated with any category. In fact, similar to 9-area splitting, with 9DSpa approach, we can build only 218 theoretically authorized codes. In DB, we have found 206 codes among these theoretical ones. In interpreting horizontally Fig.17, we see that one category C_j can be associated only to some 9DSpa codes. This information can be integrated usefully in a knowledge base dedicated to artificial vision. For example, in an image where an instance of category C_j was detected, we suppose that another category C_z can appear, and we would like localize this category. Quickly, we can give the priority only to the searching areas around C_j associated to some codes relevant with C_j . This action can reduce considerably the searching time. Interpreting vertically Fig.17, we observe that the most frequent codes are : 004 (■), 016 (■), 064 (■), 256 (■) with respectively probabilities 14%, 13%, 14%, and 13% (see distribution of 9DSpa codes in Fig.18). Furthermore, we can use the probability of each 9DSpa code for each couples of categories. Some examples about these probabilities are listed in Tab 19 of Annex C.2.

We examine now some particular examples. With category CHIMNEY, 9DSpa relationship of this reference category with others categories is resumed in Fig.19 and 40(b) of Annex C.2). In accordance

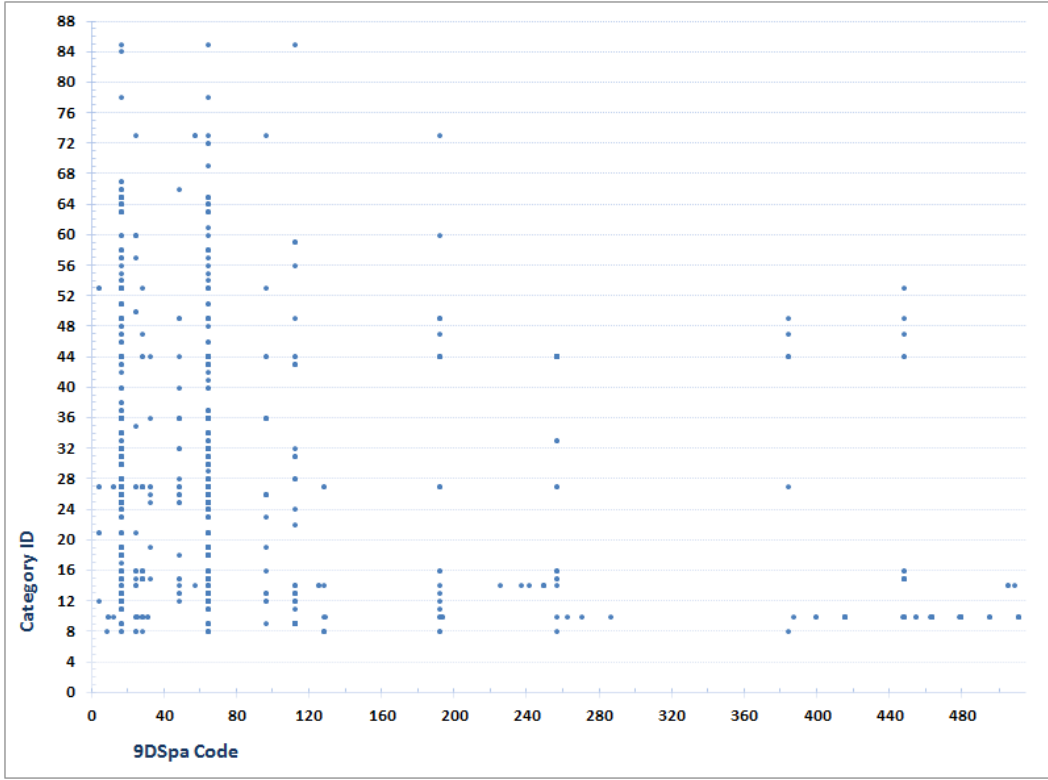


FIGURE 19 – Distribution of 9DSpa codes across categories by considering CHIMNEY as reference entity

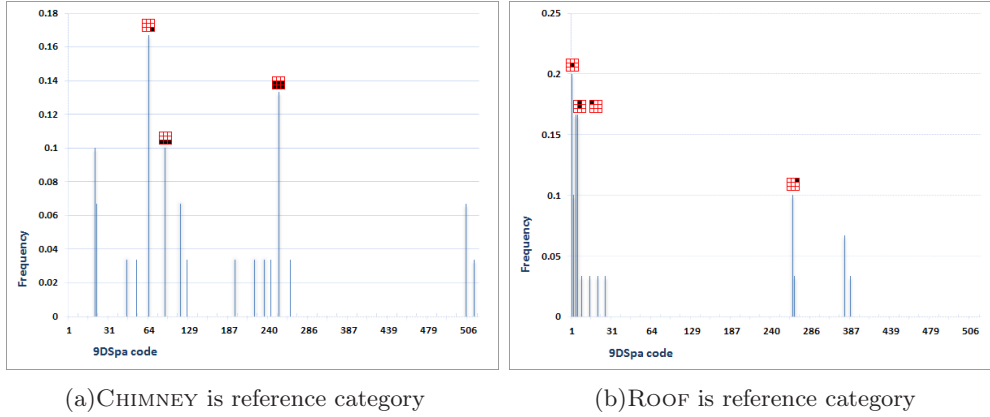





FIGURE 20 – 9DSpa relationship between category CHIMNEY and category ROOF.

with reality, the statistics show that CHIMNEY is usually above other categories. Some other examples concerning ROOF, CAR, ROAD also are cited in Fig.40 of Annex C.2. Moreover, we can study 9DSpa relationship between CHIMNEY and a particular category, for example with ROOF (see Figure 20). This couple obtains the three best probabilities of presence 0.10, 0.14 and 0.17 with respective areas ,  and . These results can provide an advantage in limiting a searching area for a target entity when knowing the location of reference one. During an object detection and localization task, this knowledge gives the possibility to constrain the search of the target object to priority searching areas in the image and to corresponding object's size, given a reference object. All the associated statistics are available

on the website² of this work.

4.2.2 Topological relationship

| Code | Label | Code | Label | Code | Label | Code | Label |
|------|----------|------|--------|------|----------|------|------------|
| (0) | disjoint | (1) | meets | (2) | overlaps | (3) | contains |
| (4) | insides | (5) | equals | (6) | covers | (7) | covered by |

TABLE 11 – Codes in topological approach.

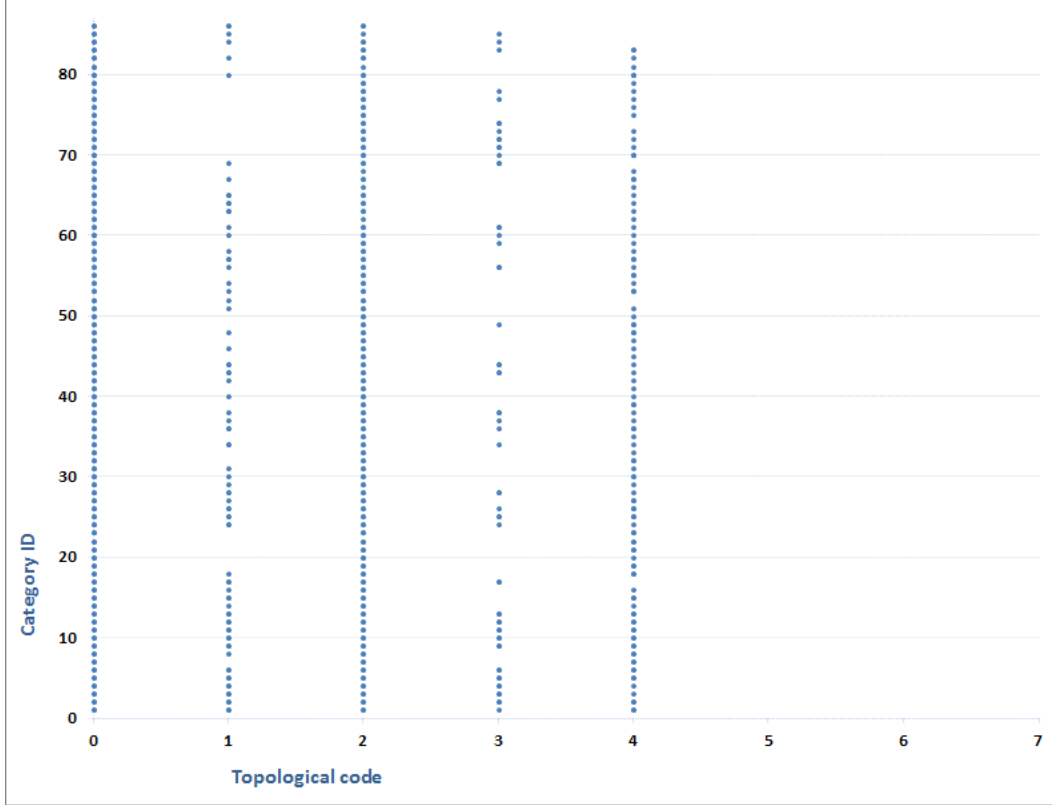


FIGURE 21 – Map of co-occurrence relationships between topological codes and categories in database.

The description of topological relationships provides eight types of relationships (represented in Table 11). We remark that, in DB, "equal", "cover", and "coverby" do not appear (see Figure 22). "Disjoint" is very frequent with a frequency more than 94%. The second position is for "overlap" with a frequency around 2.8%. "Contain" and "inside" are present only 0.7% and 1.1% consecutively. "Meet" relationship is dully represented (0.3%) : its number of occurrences is small because the notion of strict adjacency between high-level objects is not common in natural contents such those of the database and because of manual annotation. Meanwhile, in literature "meet" is a popular relationship often used with some image analysis techniques such as region segmentation that generates adjacent regions by definition, with application to specific domains, e.g. satellite imagery.

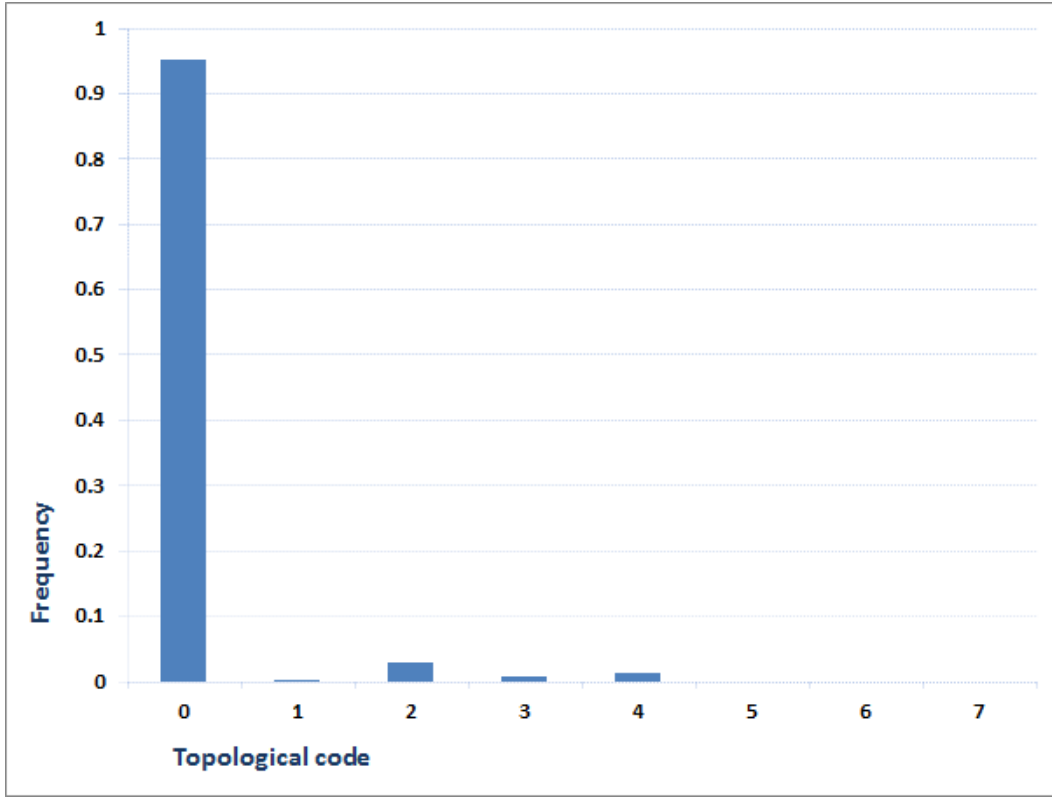
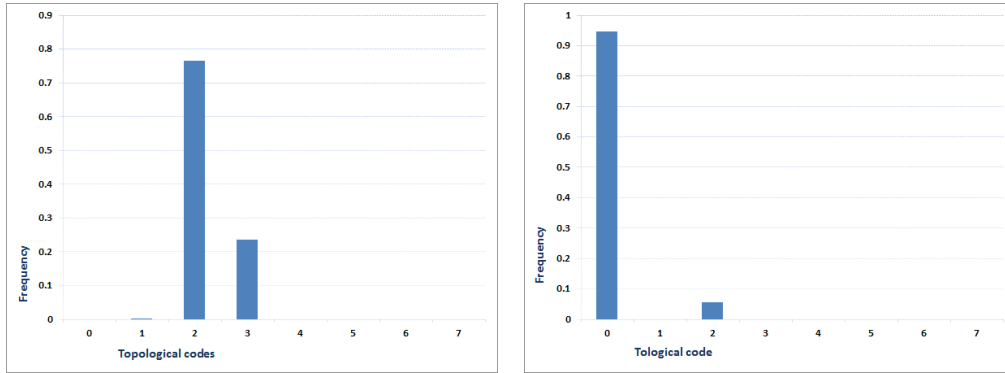


FIGURE 22 – Frequency of topological relationships in DB.



(a)ROAD - CAR. ROAD is reference category (b)CHAIR - TABLE. TABLE is reference category

FIGURE 23 – Distribution of the topological relationship between two categories for two different couples of categories.

The distribution of topological is clearly different according to couples of categories, then it can be useful in certain cases, for example in object localization. In Fig.23(a), we observed that a CAR appears mostly inside or overlaps regions occupied by a ROAD. Hence, for searching a CAR in an given image, it is possible to begin on a region of a ROAD if this last is already located. Meanwhile, "*disjoint*" information of couple TABLE-CHAIR (see Fig.23(b)) could not provide any profitable information and could complicate the searching of CHAIR based on the presence of TABLE whose size in an image may

be usually small.

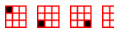

More generally, we can say that statistics on topological relationships do not provide a discriminative information. With this approach, it is difficult to get a typical interpretation or conclusion for a couple of categories, except for some special categories like ROAD and CAR. However, these statistical results can be used as a supplementary information for other approaches.

4.2.3 2D projection relationships

Similarly to topological approach, 2D projection approach is one of basic approach in image domain. The 2D projections approach associates 7 basic operators plus 6 symmetric ones (denoted by adding symbol "*" to the basic ones, see Tab 12) to each image axis, leading to 169 possible 2D relationships between MBR of entities.

| | | | | | | | | | | | | | |
|----------|---|-----|---|---|---|-----|---|---|---|----|-----|-----|-----|
| code | 1 | 2 | 3 | 4 | 5 | 6 | 7 | 8 | 9 | 10 | 11 | 12 | 13 |
| Operator | < | < * | | * | / | / * |] | [| % | = |] * | [* | % * |

TABLE 12 – codes in 2D projection approach [9].

In the same way as in previous sections, we can study co-occurrence between 2D operators and categories (see Figure 24 for x axis and Figure 25 for y axis), the frequency of occurrence of each 2D operator (see Figure 26(a) for x axis and Figure 26(b) for y axis). A concrete example is represented in Fig.27. We observe that 1D relationships |, | *,],] *, [, [* and = are not present at all on x or y axes. This result confirms that adjacency relationship is not noticeable in DB, and it also shows that 2D projections do not describe well this relationship, since they are not able to detect it here. Operators < and < * are the most frequent. It confirms partially the high frequency of "disjoint" relationship in topological approach, and moreover, of areas  with 9DSpa. In fact, operator < associated with x axis corresponds to areas  in 9DSpa. Thus, the intersection of frequencies of < and < * on axis x and y explains partially frequency of 9DSpa codes.

4.2.4 Summary of statistic

Table 13 presents a summary of the statistics obtained with DB fir the three representations of spatial relationships studied.




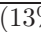
| Approach | Nb of possible relationships | Nb of effective relationships | Relationships with best occurrences (and frequency in %) |
|------------------|------------------------------|-------------------------------|---|
| 9DSpa | 511 | 206 |  (14%),  (13%),  (14%),  (13%) |
| Topological rel. | 8 | 5 | "Disjoint" (94%) |
| 2D projections | 169 | 36 | < (37%), < * (37%) (averaged on x, y axes) |

TABLE 13 – Binary spatial relationships studied and related main statistics.

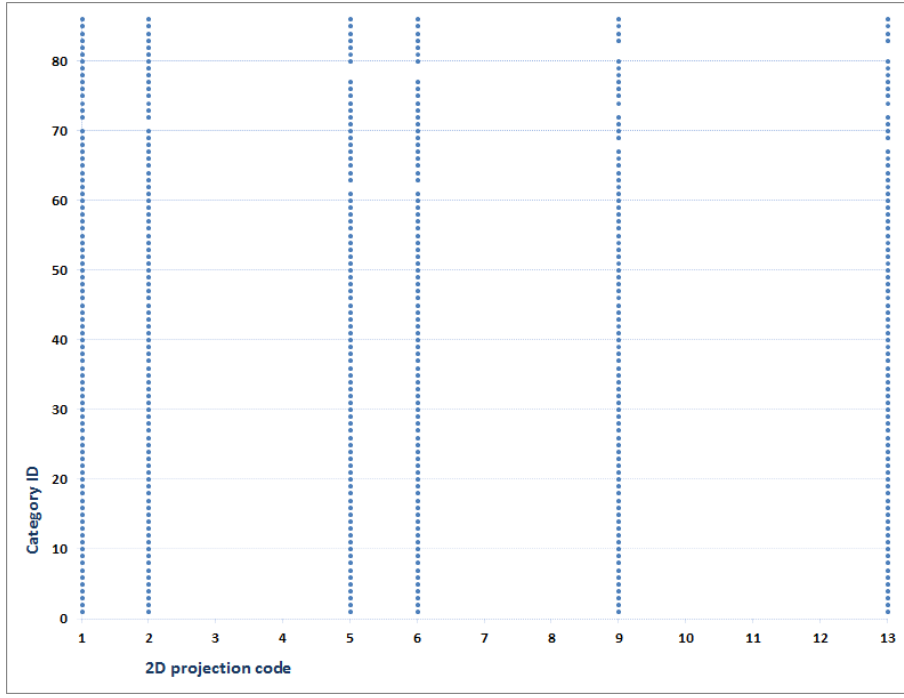


FIGURE 24 – Map of co-occurrence relationships between 2D projection operators and categories on x axis.

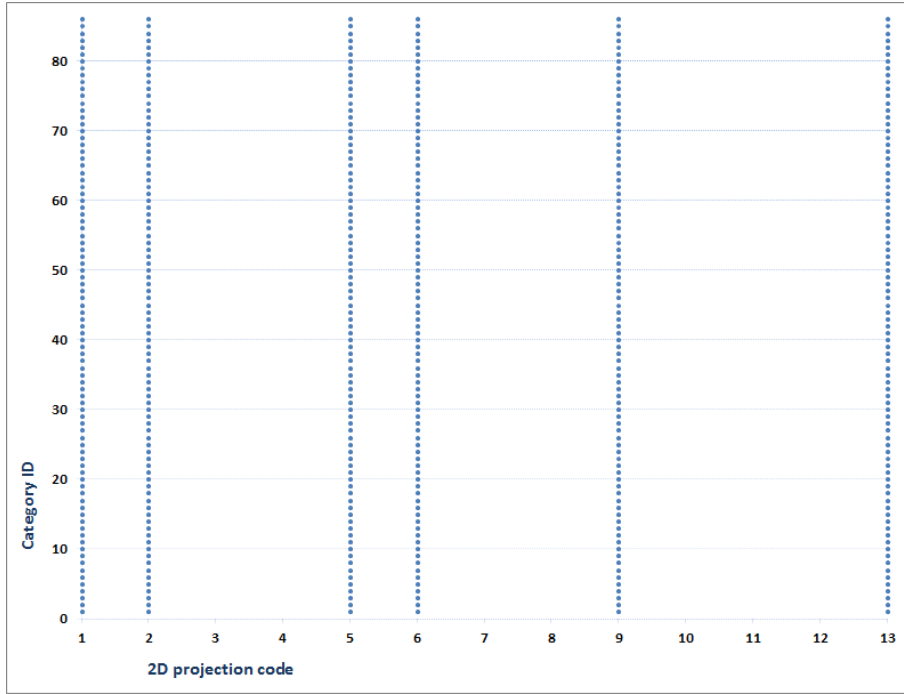


FIGURE 25 – Map of co-occurrence relationships between 2D projection operators and categories on y axis.

Among all the possible relationships existing theoretically, only a subset was effectively found in the database for each approach. The subset is particularly small with 9DSpa and 2D projections. This result

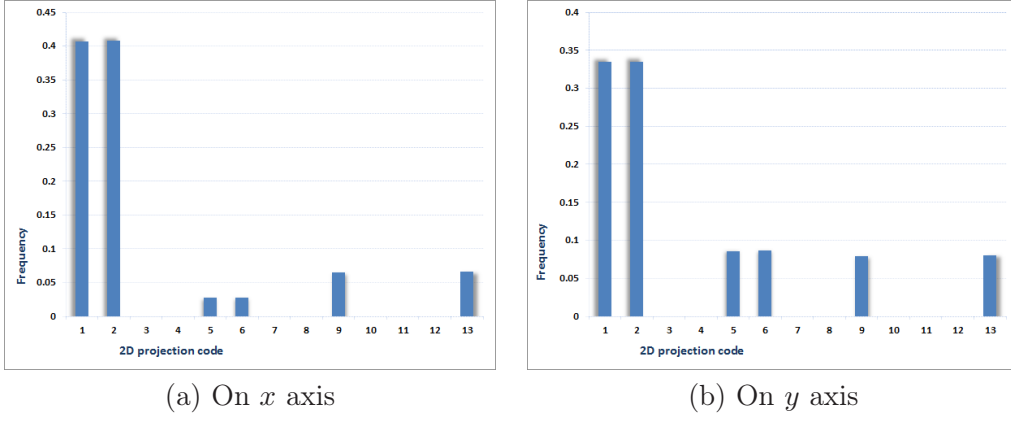


FIGURE 26 – Distribution of 2D projection codes on each image axis.

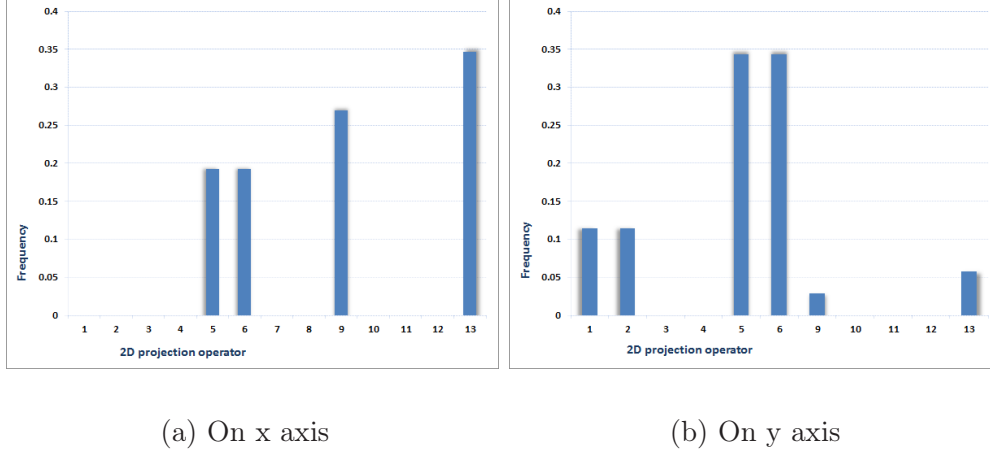


FIGURE 27 – Distribution of 2D projection relationships between SEA and MOUNTAIN.

leads to the first conclusions that the digital codes of these relationships could be optimized and that indexing them would more benefit from data driven than space driven indexes. Moreover, among these three approaches, we think that 9DSpa is the one that allows providing the most relevant statistical knowledge for future interpretations. In particular, it is possible to deduce from them the probability of presence of a given entity in an area having a given directional relationship with a reference entity, as well as an indication on its size. During an object detection and localization task, this knowledge gives the possibility to constrain the search of the target object to priority searching areas in the image and to corresponding object's size, given a reference object. All the associated statistics are available on the website² of this work.

5 Ternary relationships

A ternary relationship describes a relationship of a triplet of categories. Similarly to binary relationships, we examined co-occurrence and spatial relationships.

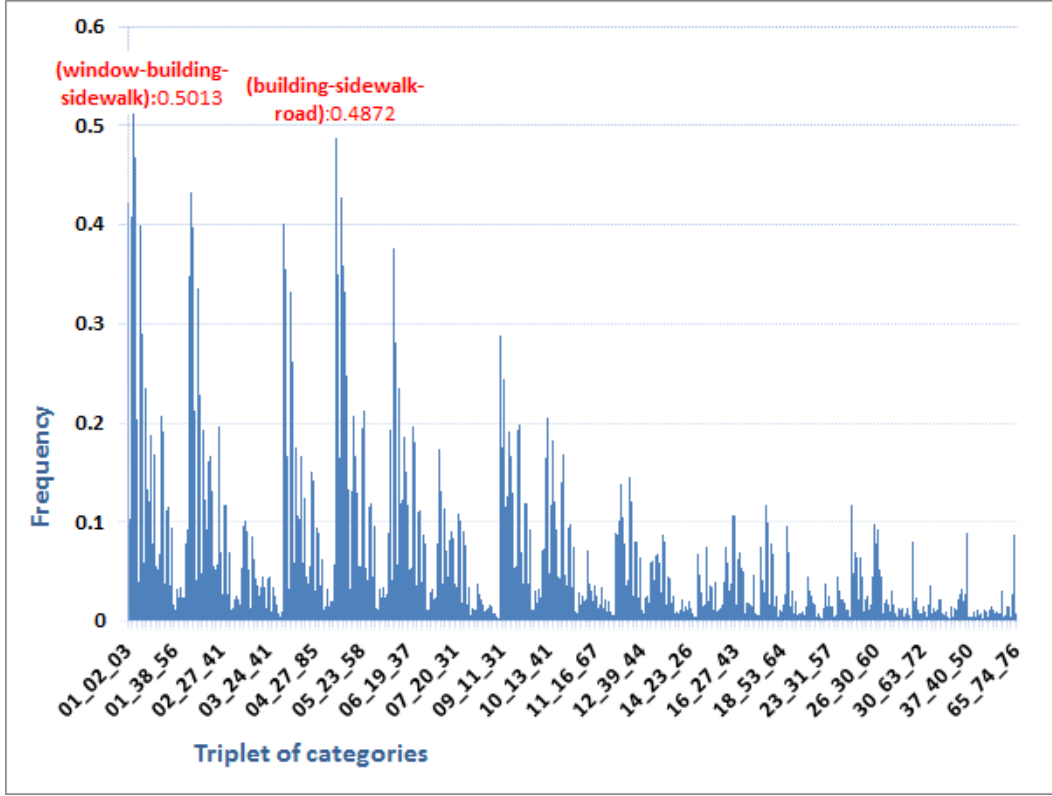


FIGURE 28 – Frequency of each triplet presence in DB.

Co-occurrence relationships

We continued to examine co-occurrence relationships for triplets of categories. We found 38031 present triplets in total knowing that we can have $C_{86}^3 = 102340$ possible triplets where order does not matter. We could compute the frequency of presence of each triplet. Fig.28 gives this frequency for each possible triplet. We observed that the most frequent triplets are (WINDOW-BUILDING-SIDEWALK) and (BUILDING-SIDEWALK-ROAD), that have frequencies of 0.5013 and 0.4872 respectively.

Then we have calculated the correlation of each triplet by adapting the basic function (see equation 1) to relationship between a category and a couple of other categories that is present in database. For a triplet $(C_j - (C_k - C_z))$, if C_j is present in image I_i , then $x_i = 1$ otherwise $x_i = 0$. If couple $(C_k - C_z)$ is present in image I_i , then $y_i = 1$ otherwise $y_i = 0$. Therefore, we examined $86 * (85 * 84 / 2) = 307020$ possible combinations. We obtained highest score 0.9891 for triplet (TORSO -(BUILDING - ARM)) and lowest score -0.2494 for triplet (WATER -(WINDOW-BUILDING)). Only 272 triplets have a correlation score more than 0.5. In Tab.14, we present the 40 triplets having highest or lowest correlation. We observed that there are the link between this correlation and correlation of couples of categories presented in previous section 4. In fact, the highest correlation in this section concerns two categories 64 (TORSO) and 65(ARM), that is the same result for correlation between couples.

To precise the analysis, we have studied the conditional probability of each triplet of categories

| 20 triplets having highest correlation | | 20 triplets having lowest correlation | |
|--|--------|--|----------|
| Triplet (A- (B-C)) | Corr. | Triplet (A- (B-C)) | Corr. |
| (TORSO - (BUILDING - ARM)) | 0.9891 | (WATER - (WINDOW - BUILDING)) | - 0.2494 |
| (ARM - (BUILDING - TORSO)) | 0.9786 | (SIDEWALK - (SKY - MOUNTAIN)) | - 0.2452 |
| (ARM - (PERSON - TORSO)) | 0.9786 | (MOUNTAIN - (BUILDING - SIDEWALK)) | - 0.2434 |
| (TORSO - (PERSON - ARM)) | 0.9784 | (BUILDING - (PLANT - FLOWER)) | - 0.2357 |
| (ARM - (HEAD - TORSO)) | 0.9732 | (BIRD - (WINDOW - BUILDING)) | - 0.235 |
| (TORSO - (HEAD - ARM)) | 0.9729 | (MOUNTAIN - (WINDOW - SIDEWALK)) | - 0.2329 |
| (ARM - (PERSON - HEAD)) | 0.9681 | (WATER - (BUILDING - SIDEWALK)) | - 0.2289 |
| (TORSO - (BUILDING - HEAD)) | 0.962 | (WATER - (BUILDING - ROAD)) | - 0.2285 |
| (ARM - (BUILDING - HEAD)) | 0.9572 | (FLOWER - (BUILDING - ROAD)) | - 0.2242 |
| (HEAD - (PERSON - ARM)) | 0.9532 | (WATER - (WINDOW - ROAD)) | - 0.2197 |
| (TORSO - (PERSON - HEAD)) | 0.9517 | (MOUNTAIN - (SIDEWALK - ROAD)) | - 0.2194 |
| (HEAD - (BUILDING - ARM)) | 0.9425 | (FLOWER - (BUILDING - SIDEWALK)) | - 0.2144 |
| (HEAD - (TORSO - ARM)) | 0.9425 | (WATER - (WINDOW - SIDEWALK)) | - 0.2144 |
| (HEAD - (BUILDING - TORSO)) | 0.9372 | (BIRD - (BUILDING - SIDEWALK)) | - 0.2143 |
| (HEAD - (PERSON - TORSO)) | 0.9372 | (BIRD - (BUILDING - ROAD)) | - 0.2141 |
| (TORSO - (WINDOW - ARM)) | 0.9217 | (BIRD - (BUILDING - SKY)) | - 0.2122 |
| (TORSO - (SIDEWALK - ARM)) | 0.9217 | (FLOWER - (WINDOW - BUILDING)) | - 0.2119 |
| (ARM - (WINDOW - TORSO)) | 0.9127 | (FLOWER - (BUILDING - SKY)) | - 0.2119 |
| (ARM - (SIDEWALK - TORSO)) | 0.9127 | (WATER - (SIDEWALK - ROAD)) | - 0.2093 |
| (TORSO - (WINDOW - HEAD)) | 0.8989 | (FLOWER - (SIDEWALK - ROAD)) | - 0.2055 |

TABLE 14 – The highest and lowest correlations between triplets of categories.

by using this function $P(A|B \cap C) = \frac{P(A \cap B \cap C)}{P(B \cap C)}$. Differently to correlation evaluation, we examined conditional probability with only triplets appearing in database. There are $38031 * 3 = 114093$ possible triplets where order matter. We found 11262 triplets having score 1. We can explain partially this result from the binary conditional probability results. In previous section on binary study, we obtained 66 conditional probabilities equal to 1. We know that $P(A|B) = 1$ when $P(A \cap B) = P(B)$, then we can say :

$$A \cap B = B \quad (6)$$

$$\Rightarrow B \subset A \quad (7)$$

$$\Rightarrow \forall C | B \cap C \neq \emptyset : (B \cap C) \subset A \quad (8)$$

$$\Rightarrow A \cap B \cap C = B \cap C \quad (9)$$

$$\Rightarrow P(A \cap B \cap C) = P(B \cap C) \quad (10)$$

$$\Rightarrow P(A|B \cap C) = 1 \quad (11)$$

For each couple (A, B) having $P(A|B) = 1$, by combining it with a category $C | C \neq B \wedge C \neq A$, we can obtain $66 * 84 = 5544$ new probabilities of 1. Alternatively, we observed that, with a couple (A, B) having $P(A|B) \simeq 1$, we can have also a high probability to obtain : $\forall C | B \cap C \neq \emptyset : (B \cap C) \subset A$. It explains why there are a high number of score 1. In this statistic, we saw also that more than 20000 triplets have a score more than 0.6. We mention related statistics in Tab.15. For more detailed results,

we would invite you to consult our website⁴.

| 20 triplets having highest P | | 20 triplets having lowest P | |
|--------------------------------|-------|-------------------------------|--------|
| Triplet (A- (B-C)) | Prob. | Triplet (A- (B-C)) | Prob. |
| WINDOW - (CAR -WIRE) | 1 | LEAF - (WINDOW -BUILDING) | 0.0013 |
| WINDOW - (CAR -ROCK) | 1 | HAT - (WINDOW -BUILDING) | 0.0013 |
| WINDOW - (CAR -RAILING) | 1 | LAKE - (BUILDING -ROAD) | 0.0014 |
| WINDOW - (CAR -GRILLE) | 1 | LEAF - (BUILDING -ROAD) | 0.0014 |
| WINDOW - (CAR -LAMP) | 1 | HAT - (BUILDING -ROAD) | 0.0014 |
| WINDOW - (CAR -LIGHT) | 1 | BOAT - (BUILDING -SIDEWALK) | 0.0015 |
| WINDOW - (CAR -POT) | 1 | WATER - (BUILDING -SIDEWALK) | 0.0015 |
| WINDOW - (CAR -PIPE) | 1 | LEAF - (BUILDING -SIDEWALK) | 0.0015 |
| WINDOW - (CAR -FIRE ESCAPE) | 1 | DUCK - (BUILDING -SKY) | 0.0015 |
| WINDOW - (CAR -CHAIR) | 1 | LEAF - (BUILDING -SKY) | 0.0015 |
| WINDOW - (CAR -MAILBOX) | 1 | HAT - (BUILDING -SKY) | 0.0015 |
| WINDOW - (CAR -FLOWER) | 1 | BOAT - (WINDOW -ROAD) | 0.0015 |
| WINDOW - (CAR -CROSS WALK) | 1 | SEA - (WINDOW -ROAD) | 0.0015 |
| WINDOW - (CAR -CONE) | 1 | WATER - (WINDOW -ROAD) | 0.0015 |
| WINDOW - (CAR -TABLE) | 1 | LEAF - (WINDOW -ROAD) | 0.0015 |
| WINDOW - (CAR -UMBRELLA) | 1 | HAT - (WINDOW -ROAD) | 0.0015 |
| WINDOW - (CAR -SAND) | 1 | BOAT - (WINDOW -SIDEWALK) | 0.0016 |
| WINDOW - (CAR -WATER) | 1 | SEA - (WINDOW -SIDEWALK) | 0.0016 |
| WINDOW - (CAR -ATTIC) | 1 | WATER - (WINDOW -SIDEWALK) | 0.0016 |

TABLE 15 – The highest and lowest conditional probabilities between triplets of categories.

Ternary spatial relationships

In last years, to our knowledge, a few approaches were proposed to describe triangular relationships of three symbolic entities. We can mention TSR approach [5] and our approach Δ -TSR [6]. By applying to a set of heterogeneous symbolic entities that do not have fixed shape and size, these approaches cannot described finally triangular spatial relationships between symbolic entities since they take into account only the center of each entity as representation of it. However, to complete this study, based on the theory of Δ -TSR, we have studies the relationships between three different categories by using Δ -TSR_{3D}. This description is invariant to translation, 2D rotation, scale, and flip. Triangular relationships are built on the centers of three entities. The first component of Δ -TSR_{3D} is the identification of the triplet of categories, the second and the third components are consecutively the first and the second angles of triangle obtained from the three centers. They correspond to angles a_1 and a_2 in Fig.32.

Firstly, we present a general vision on approach's second component in all DB with Fig. 29 and 30. We observed that this component is distributed quasi homogeneously in interval [0..180]. Then, with the ternary relationship, we can say it is complex to give a direct interpretation, for example to predict an area of searching, by using simply an angle. Although, this relationship can be useful for a representation fuzzy relationship like "between" relationship. Suppose that we do not take into account

4. <http://www.lamsade.dauphine.fr/~hoang/www/cartography>

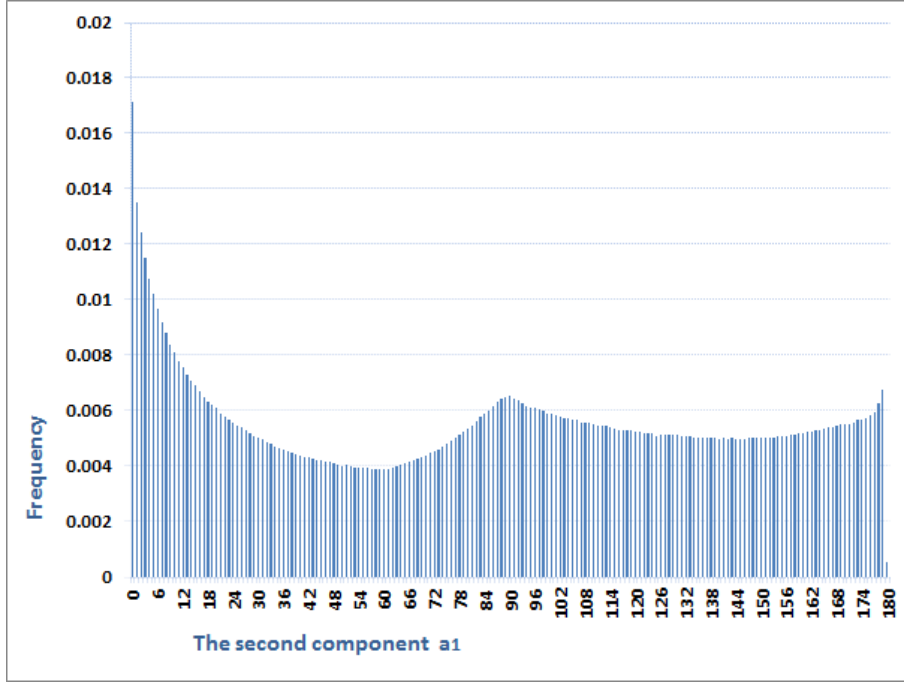


FIGURE 29 – Statistics of second component of $\Delta-TSR_{3D}$.

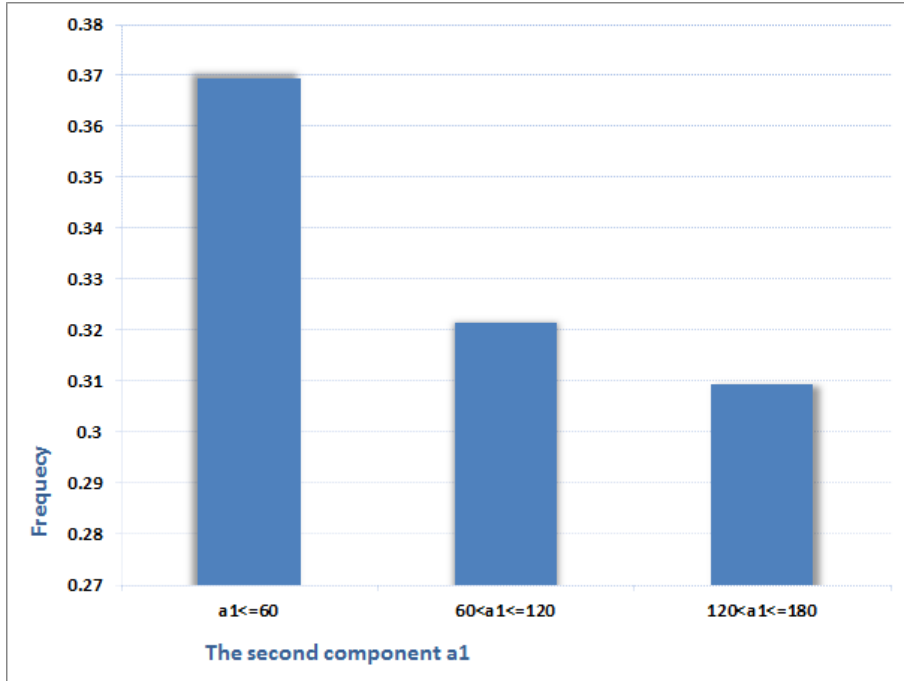


FIGURE 30 – Resume of statistics of second component of $\Delta-TSR_{3D}$.

the shape of category's instance, the "between" relationship can be used by restricting the value of the two angles in $\Delta-TSR_{3D}$. For example, a third entity C_3 can be viewed "between" C_1 and C_2 when $a_1 \leq 60$ and $a_2 \leq 60$ (see Figure 31). If we take into account the entity's shape, we can combine the 9DSpa approach with $\Delta-TSR_{3D}$ to get a definition more complete of "between" relationship. We

have computed the probability of the third category to be "between" the two first categories in triplet (see Figure 32). We found 3376 triplets having probability score more than 0.5. For example, when we find a SIDEWALK and a CHAIR in an image, if there is a MOTOBIKE in this image, we could believe that this MOTOBIKE would be probably "between" these two first entities since the corresponding probability is 0.978. In the same way, the same study for the first or second category in triple can be done easily.

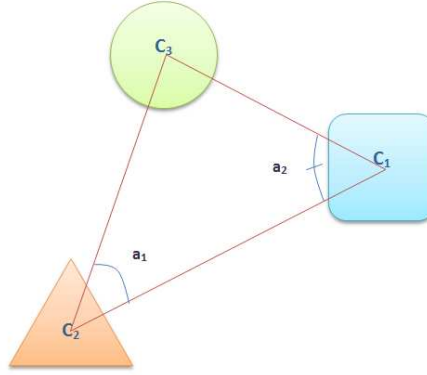


FIGURE 31 – Illustration of relationship "between" : Category C_3 is between two other categories in $\Delta-TSR_{3D}$.

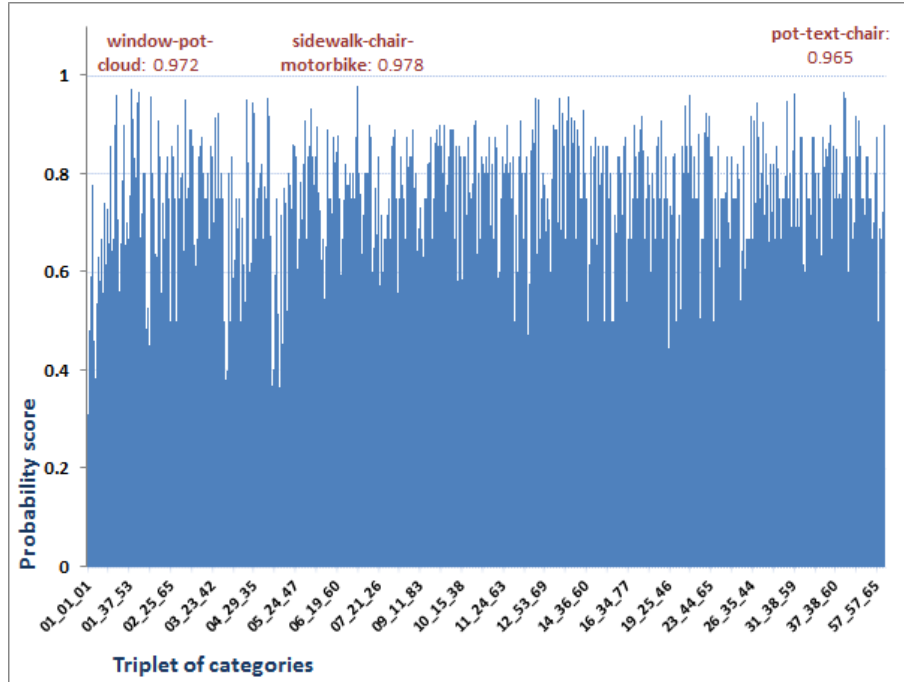


FIGURE 32 – Category triplets satisfying "between" relationship with $\Delta-TSR_{3D}$.

Because of limits of the spatial representation of ternary relationships for symbolic entities, we did not conduct additional statistical study on this type relationship. Δ -TSR provided more many advantages with low level feature like interest points. We think that this approach can be relevant for symbolic entities if we know how to associate other contextual information of category to it. It can

surely be done in some domains like medical domain where Δ -TSR could show its ability on homogeneous entities having a fixed size and shape.

6 Conclusion

We have presented a statistical study on spatial relationships of categories of entities from a public database of annotated images. This study provides a cartography of the spatial relationships that can be encountered in a database of heterogeneous natural contents. We think that it could be integrated with benefit in a knowledge-based system dedicated to artificial vision and CBIR, in order to enrich the description of the visual content as well as to help to choose the most discriminant type of relationships for each use case. Here, we have focussed on the analysis of unary, binary, and ternary relationships. Study on unary relationships highlights trends on location of categories of entities in the image. These measures allows to determine the probability of the presence of a category in a given area, and to perform spatial reasoning. In the same way, study on binary relationships allows deducing the probability of presence of a category in an area regarding the location of another reference category. In addition, it gives indications on the relevance of the tested representations of these relationships. Ternary spatial relationships were already studied. Because of limits of the spatial representation of ternary relationships for symbolic entities, we did not conduct deeper statistical study on this type relationship.

This work was done on a manually annotated database of one thousand images. Therefore, it is evident that these statistics will have to be confirmed or refined on other image databases of larger size. However from now, we think that these measures can help us, on the one hand, to better understand which kinds of spatial relationship should be employed for a given problem and how to model them. On the other hand, such statistics can help to start a knowledge base on these relationships, that can be applied quickly to some topical problems of artificial vision and CBIR such as object detection, recognition or retrieval in a collection.

References

- [1] C. Chang. Spatial match retrieval of symbolic pictures. *Journal of Information Science and Engineering*, 7(3) :405–422, 1991. 20
- [2] S.-K. Chang and E. Jungert. A spatial knowledge structure for image information systems using symbolic projections. *IJCC*, 1986. 20
- [3] M. J. Egenhofer and K. K. Al-Taha. Reasoning about gradual changes of topological relationships. In *Proc. of the International Conference GIS*, pages 196–219, London, UK, 1992. Springer-Verlag. 1, 20
- [4] V. Gouet-Brunet, M. Manouvrier, and M. Rukoz. Synthèse sur les modèles de représentation des relations spatiales dans les images symboliques. *RNTI*, (RNTI-E-14) :19–54, 2008. 1, 20
- [5] D. Guru, P. Punitha, and P. Nagabhushan. Archival and retrieval of symbolic images : An invariant scheme based on triangular spatial relationship. *Pattern Recognition Letters*, 24(14) :2397–2408, 2003. 31
- [6] N. V. Hoàng, V. Gouet-Brunet, M. Rukoz, and M. Manouvrier. Embedding spatial information into image content description for scene retrieval. *Pattern Recognition*, 43(9) :3013–3024, 2010. 31
- [7] P. Huang and C. Lee. Image Database Design Based on 9D-SPA Representation for Spatial Relations. *TKDE*, 16(12) :1486–1496, 2004. 1, 20
- [8] D. Mayhew. *Principles and guidelines in software user interface design*. Prentice-Hall, 1992. 11
- [9] M. Nabil, J. Shepherd, and A. H. H. Ngu. 2D projection interval relationships : A symbolic representation of spatial relationships. In *Symposium on Large Spatial Databases*, pages 292–309, 1995. 20, 26
- [10] J. Nogier. *Ergonomie du logiciel et design Web*. Dunod, 2005. 11
- [11] J. Park, V. Govindaraju, and S. N. Srihari. Genetic engineering of hierarchical fuzzy regional representations for handwritten character recognition. *International Journal on Document analysis and recognition*, 2000. 8
- [12] B. Russell, A. Torralba, K. Murphy, and W. Freeman. Labelme : a database and web-based tool for image annotation. In *Proc. of the International Journal of Computer Vision*, Volume 177(Issue 1-3) :157–173, 2008. 2
- [13] W. Wang, A. Zhang, and Y. Song. Identification of objects from image regions. *Int. Conf. on Multimedia and Expo*, 2003. 8

A Annotated image database

A.1 Statistics on categories

| Categ. ID | Corr. | Categ. ID | Corr. | Categ. ID | Corr. | Categ. ID | Corr. |
|-----------|-------|-----------|-------|-----------|-------|-----------|-------|
| 01 | 0.776 | 23 | 0.230 | 45 | 0.093 | 67 | 0.11 |
| 02 | 0.664 | 24 | 0.225 | 46 | 0.044 | 68 | 0.131 |
| 03 | 0.248 | 25 | 0.495 | 47 | 0.211 | 69 | 0.117 |
| 04 | 0.652 | 26 | 0.568 | 48 | 0.178 | 70 | 0.145 |
| 05 | 0.637 | 27 | 0.231 | 49 | 0.319 | 71 | 0.030 |
| 06 | 0.548 | 28 | 0.238 | 50 | 0.131 | 72 | 0.077 |
| 07 | 0.303 | 29 | 0.191 | 51 | 0.231 | 73 | 0.136 |
| 08 | 0.169 | 30 | 0.351 | 52 | 0.121 | 74 | 0.000 |
| 09 | 0.107 | 31 | 0.232 | 53 | 0.287 | 75 | 0.102 |
| 10 | 0.057 | 32 | 0.371 | 54 | 0.134 | 76 | 0.137 |
| 11 | 0.253 | 33 | 0.220 | 55 | 0.217 | 77 | 0.106 |
| 12 | 0.528 | 34 | 0.247 | 56 | 0.115 | 78 | 0.126 |
| 13 | 0.400 | 35 | 0.234 | 57 | 0.181 | 79 | 0.109 |
| 14 | 0.192 | 36 | 0.641 | 58 | 0.299 | 80 | 0.125 |
| 15 | 0.379 | 37 | 0.147 | 59 | 0.124 | 81 | 0.107 |
| 16 | 0.405 | 38 | 0.144 | 60 | 0.299 | 82 | 0.059 |
| 17 | 0.121 | 39 | 0.118 | 61 | 0.091 | 83 | 0.163 |
| 18 | 0.316 | 40 | 0.186 | 62 | 0.044 | 84 | 0.207 |
| 19 | 0.343 | 41 | 0.103 | 63 | 0.304 | 85 | 0.122 |
| 20 | 0.098 | 42 | 0.133 | 64 | 0.295 | 86 | 0.029 |
| 21 | 0.242 | 43 | 0.266 | 65 | 0.304 | | |
| 22 | 0.141 | 44 | 0.315 | 66 | 0.118 | | |

TABLE 16 – Inter-class correlation of 86 categories.

B Unary relationships

B.1 Results analysis

We were interested how to define the function allowing to determinate the theoretically authorized codes from a set of initial ones (the smallest atomic ones). Suppose that an image I is splitted in n atomic areas A_s . The code representing A_s is noted $cod(A_s)$. The set of areas that are joint by edge with A_s is noted $edge(A_s)$. For two atomic areas A_{s_i} and A_{s_j} , we call $comb(A_{s_i}, A_{s_j})$ the function combining these two areas to give a new complex area.

$$comb(A_{s_i}, A_{s_j}) = \begin{cases} null & \text{if } A_{s_j} \notin edge(A_{s_i}) \\ A_k | A_k = A_{s_i} \cup A_{s_j} & \text{otherwise} \end{cases} \quad (12)$$

with :

$$cod(A_k) = cod(A_{s_i}) + cod(A_{s_j}) \quad (13)$$

$$edge(A_k) = edge(A_{s_i}) \cup edge(A_{s_j}) \setminus \{A_{s_i}, A_{s_j}\} \quad (14)$$

Now, we can define the function FC allowing to indicate all theoretically authorized areas from a set of two atomic areas.

$$FC(\{A_{s_i}, A_{s_j}\}) = \{A_{s_i}, A_{s_j}, comb(A_{s_i}, A_{s_j})\} \quad (15)$$

Suppose that we have a set A_i a complex area containing more than two atomic areas, then, we can define recursively the function FC on A_i :

$$FC(A_i) = FC(\{A_{s_i}, F_t(A_i / \{A_{s_i}\})\}) \quad (16)$$

$$= \{FC(\{A_{s_i}, A_k | A_k \in FC(A_i / \{A_{s_i}\})\})\} \quad (17)$$

See examples of $FC(A_i)$ in Tab.17 for building vertical/horizontal line, border or center area with each type of splitting.

| | A_i | $F(A_i)$ |
|---------------|-------------------------------|---|
| 9-area codes | {1, 8, 9} | {1, 8, 64, 9, 72, 73} |
| | {2, 16, 128} | {2, 16, 128, 18, 144, 146} |
| | {4, 32, 256} | {4, 32, 256, 36, 288, 292} |
| | {1, 2, 4} | {1, 2, 4, 3, 6, 7} |
| | {8, 16, 32} | {8, 16, 32, 24, 48, 56} |
| | {64, 128, 256} | {64, 128, 256, 192, 384, 448} |
| 16-area codes | {1, 16, 256, 4096} | {1, 16, 256, 4096, 17, 272, 4352, 273, 4368, 4369} |
| | {2, 32, 512, 8192} | {2, 32, 512, 8192, 34, 544, 8704, 546, 8736, 8738} |
| | {4, 64, 1024, 16384} | {4, 64, 1024, 16384, 68, 1088, 17408, 1092, 17472, 17476} |
| | {8, 128, 2048, 32768} | {8, 128, 2048, 32768, 136, 2176, 34816, 2184, 34944, 34952} |
| | {1, 2, 4, 8} | {1, 2, 4, 8, 3, 6, 12, 7, 14, 15} |
| | {16, 32, 64, 128} | {16, 32, 64, 128, 48, 96, 192, 112, 224, 240} |
| | {256, 512, 1024, 2048} | {256, 512, 1024, 2048, 768, 1536, 3072, 1792, 3584, 3840} |
| | {4096, 8192, 16384, 32768} | {4096, 8192, 16384, 32768, 12288, 24576, 49152, 28672, 57344, 61440} |
| | {32, 64, 112, 224, 512, 1024} | {32, 64, 96, 512, 544, 608, 1024, 1088, 1120, 1536, 1632} |
| | The border area | { 1, 2, 3, 4, 6, 7, 8, 12, 14, 15, 16, 17, 19, 23, 31, 128, 136, 140, 142, 143, 159, 256, 272, 273, 275, 279, 287, 415, 2048, 2176, 2184, 2188, 2190, 2191, 2207, 2463, 4096, 4352, 4368, 4369, 4371, 4375, 4383, 4511, 6559, 8192, 12288, 12544, 12560, 12561, 12563, 12567, 12575, 12703, 14751, 16384, 24576, 28672, 28928, 28944, 28945, 28947, 28951, 28959, 29087, 31135, 32768, 34816, 34944, 34952, 34956, 34958, 34959, 34975, 35231, 39327, 47519, 49152, 51200, 51328, 51336, 51340, 51342, 51343, 51359, 51615, 55711, 57344, 59392, 59520, 59528, 59532, 59534, 59535, 59551, 59807, 61440, 61696, 61712, 61713, 61715, 61719, 61727, 61855, 63488, 63616, 63624, 63628, 63630, 63631, 63647, 63744, 63760, 63761, 63763, 63767, 63775, 63872, 63880, 63884, 63886, 63887, 63888, 63889, 63891, 63895, 63896, 63897, 63899, 63900, 63901, 63902, 63903 } |

TABLE 17 – Sets of codes presenting a location on horizontal/vertical line in image.

C Binary relationships

C.1 Co-occurrence relationships

| Cat.ID | 01 | 02 | 05 | 06 | 10 | 13 | 16 | 20 | 28 | 34 | 43 | 74 | 85 |
|--------|--------|--------|--------|--------|--------|--------|--------|--------|--------|--------|--------|--------|-------|
| 01 | 0.776 | | | | | | | | | | | | |
| 02 | 0.609 | 0.664 | | | | | | | | | | | |
| 05 | 0.788 | 0.566 | 0.637 | | | | | | | | | | |
| 06 | 0.733 | 0.613 | 0.696 | 0.548 | | | | | | | | | |
| 10 | 0.275 | 0.2 | 0.35 | 0.209 | 0.057 | | | | | | | | |
| 13 | 0.124 | 0.13 | 0.059 | 0.111 | -0.024 | 0.4 | | | | | | | |
| 16 | 0.363 | 0.371 | 0.376 | 0.371 | 0.245 | 0.066 | 0.405 | | | | | | |
| 20 | 0.043 | 0.071 | 0.026 | 0.036 | 0.071 | 0.072 | -0.005 | 0.098 | | | | | |
| 28 | 0.191 | 0.132 | 0.174 | 0.167 | 0.12 | 0.117 | 0.083 | 0.047 | 0.238 | | | | |
| 34 | 0.154 | 0.104 | 0.153 | 0.128 | 0.113 | 0.049 | 0.151 | 0.087 | 0.248 | 0.247 | | | |
| 43 | -0.13 | -0.066 | -0.035 | -0.132 | 0.072 | 0.039 | 0.053 | -0.041 | 0.003 | 0.009 | 0.266 | | |
| 74 | -0.149 | -0.097 | -0.117 | -0.133 | 0.007 | -0.063 | -0.045 | -0.012 | -0.032 | -0.031 | 0.163 | 0 | |
| 85 | -0.071 | -0.033 | -0.008 | -0.112 | 0.092 | -0.069 | -0.052 | -0.013 | -0.005 | -0.033 | -0.013 | -0.015 | 0.122 |

TABLE 18 – Correlation scores of some couples of categories in DB. The scores on the diagonal represent the inter-class correlation.

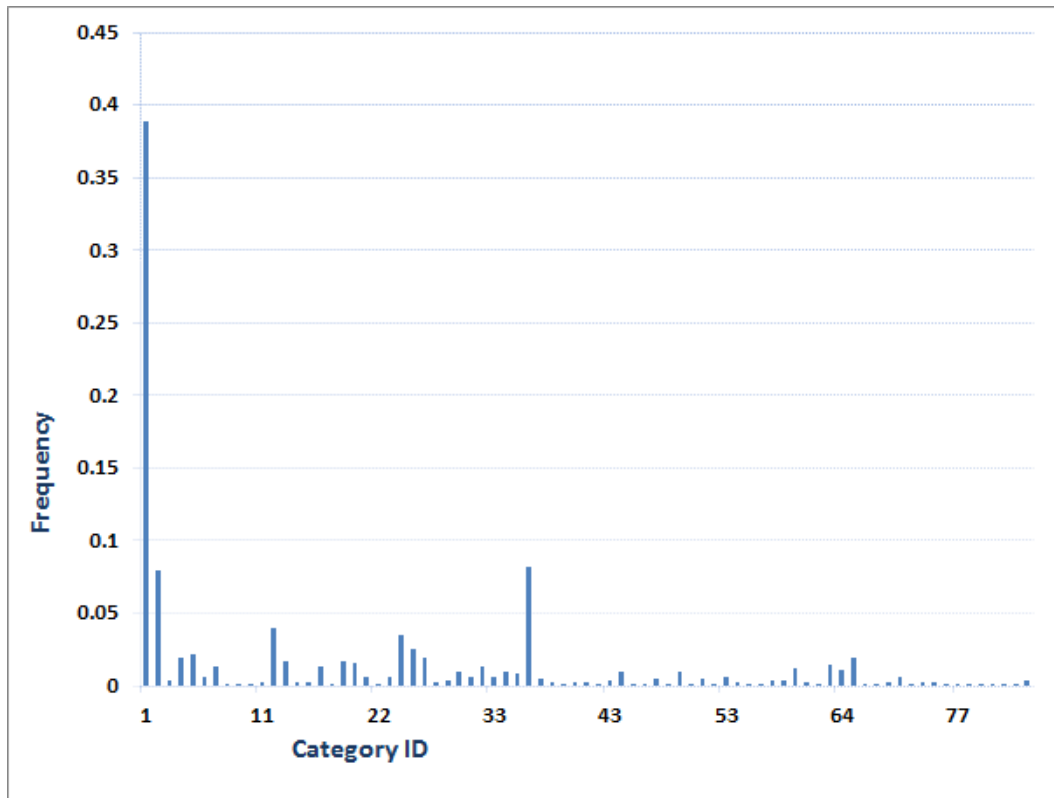


FIGURE 33 – Distribution of categories according to code 16 in 9-area splitting.

C.2 Binary spatial relationships

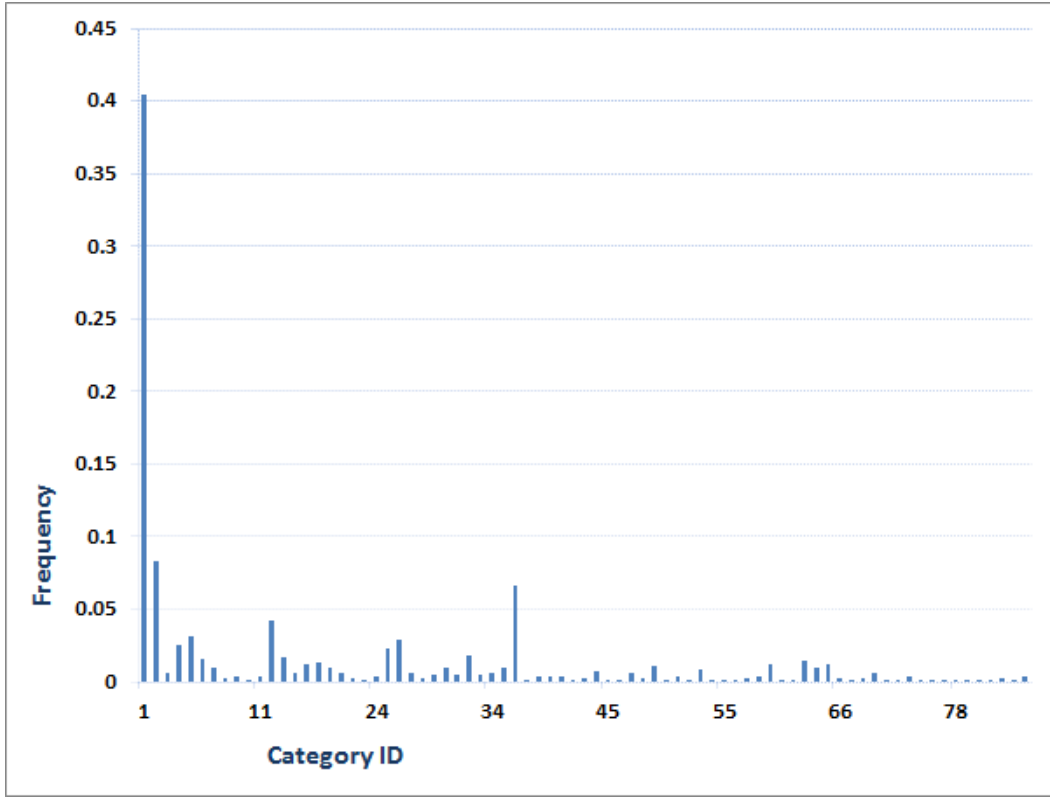


FIGURE 34 – Distribution of categories according to code 128 in 9-area splitting.

| Cat. ID 01 | Cat. ID 02 | 9Dspa code | Number of occ. |
|------------|------------|------------|----------------|
| 01 | 02 | 16 | 21774 |
| 02 | 01 | 256 | 21774 |
| 01 | 02 | 64 | 19349 |
| 02 | 01 | 4 | 19349 |
| 01 | 36 | 64 | 18852 |
| 36 | 01 | 4 | 18852 |
| 01 | 36 | 16 | 17934 |
| 36 | 01 | 256 | 17934 |
| 01 | 26 | 64 | 16626 |
| 26 | 01 | 4 | 16626 |
| 01 | 26 | 16 | 16337 |
| 26 | 01 | 256 | 16337 |
| 05 | 01 | 1 | 13334 |
| 01 | 05 | 511 | 11702 |
| 09 | 01 | 2 | 11640 |
| 01 | 09 | 112 | 11598 |
| 06 | 01 | 2 | 8222 |
| 01 | 06 | 112 | 8176 |
| 01 | 12 | 16 | 7084 |
| 12 | 01 | 256 | 7084 |

TABLE 19 – 20 couples of categories the most frequent by 9Dspa codes.

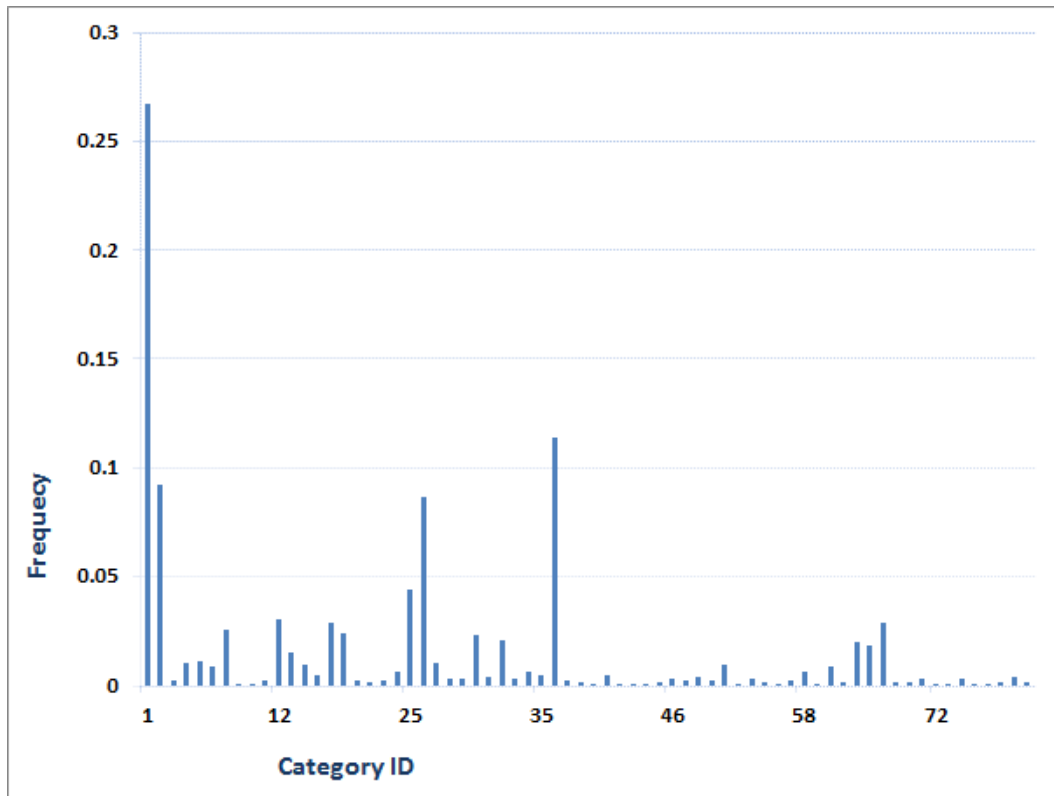


FIGURE 35 – Distribution of categories according to code 1024 in 16-area splitting.

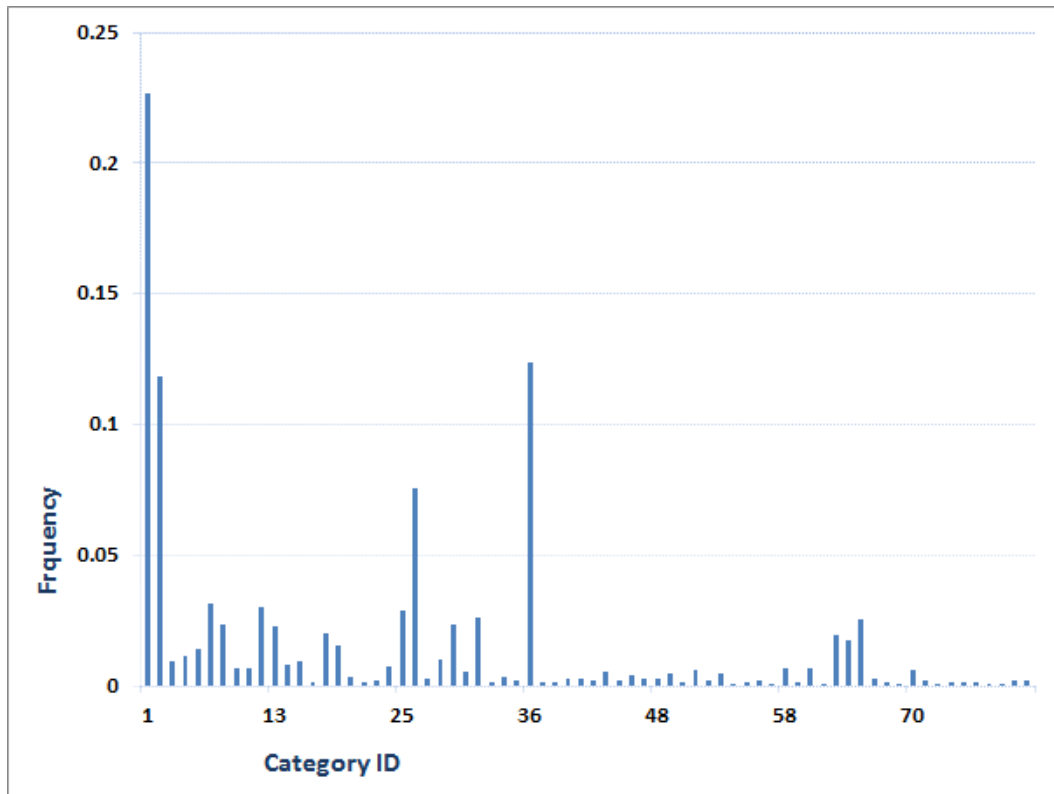


FIGURE 36 – Distribution of categories according to code 16384 in 16-area splitting.

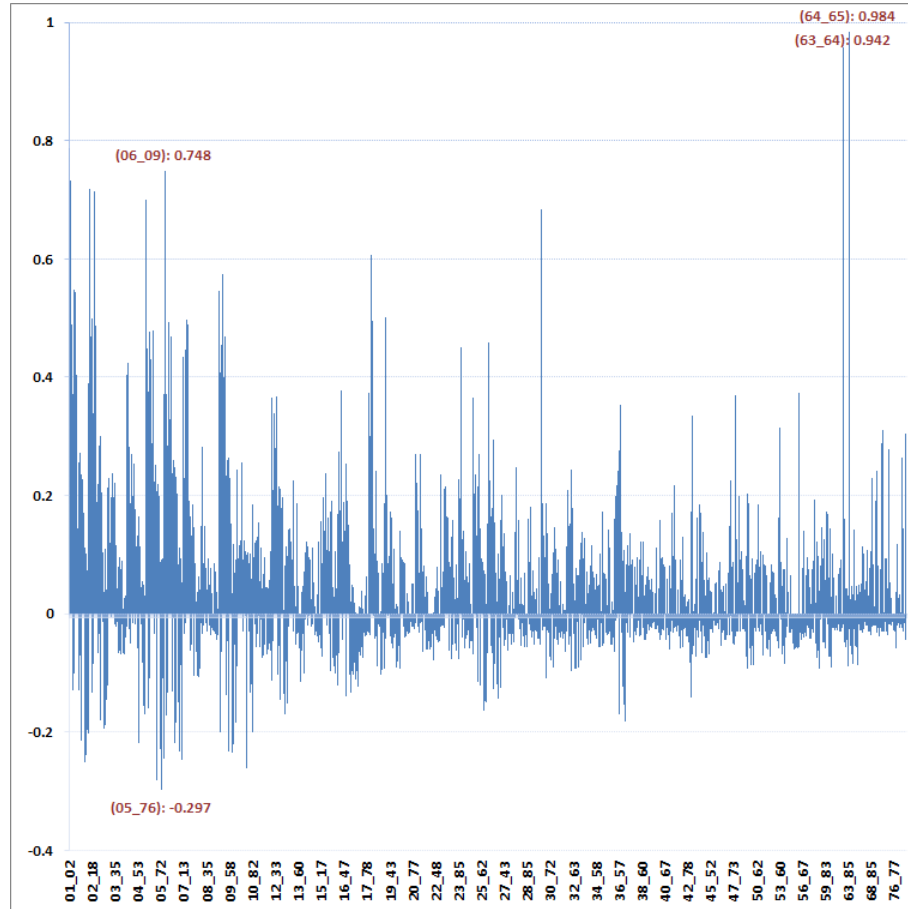


FIGURE 37 – Distribution of correlation for every category pairs in DB.

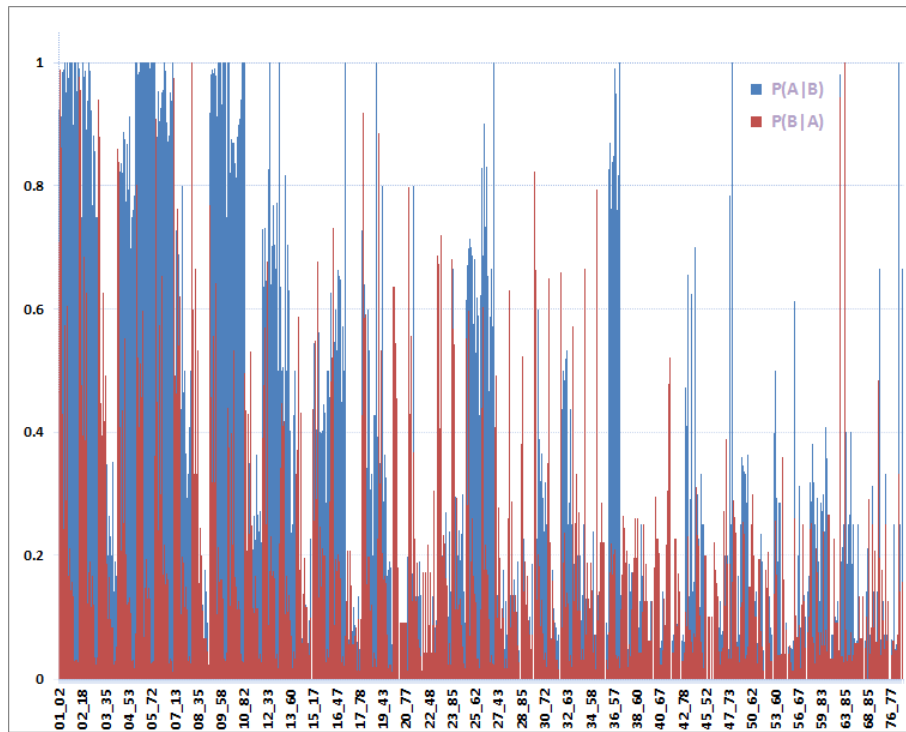


FIGURE 38 – Distribution of conditional probabilities for every category pairs in DB.

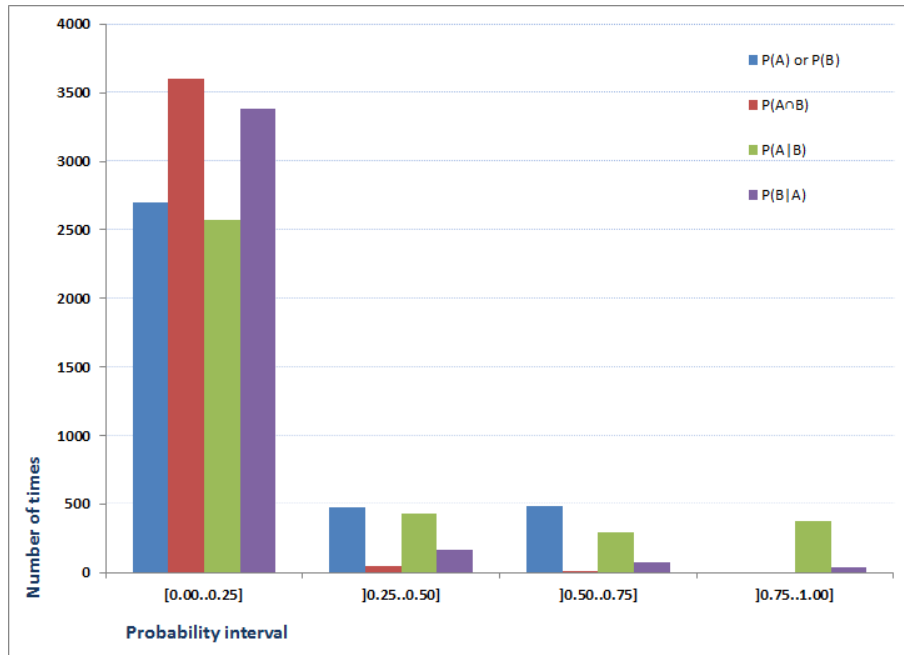
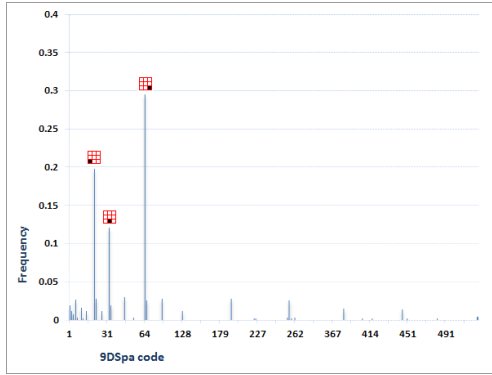
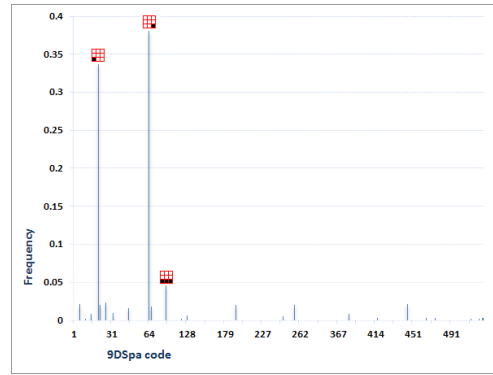


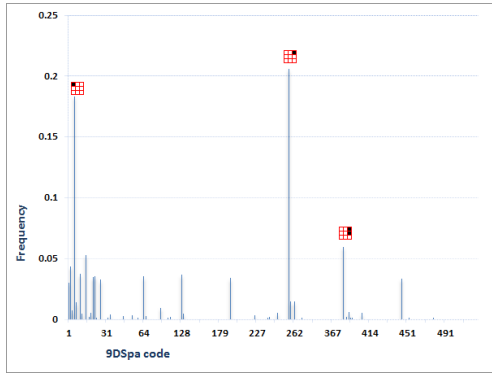
FIGURE 39 – Overview of all probabilities in DB.



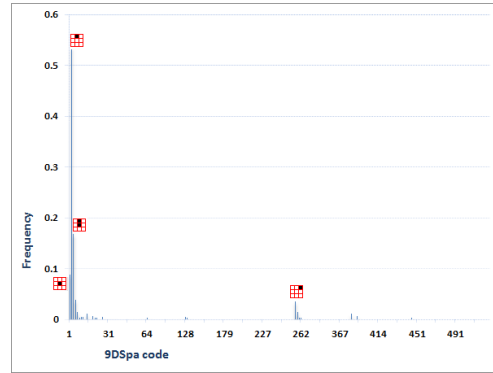
(a) ROOF is reference category



(b) CHIMNEY is reference category



(c) CAR is reference category



(d) ROAD is reference category

FIGURE 40 – Examples of statistical study on 9DSpa relationships between a reference category and others.